KAPITAŁ LUDZKI
NARODOWA STRATEGIA SPÓJNOŚCI

Politechnika Wrocławska

UNIA EUROPEJSKA
EUROPEJSKI
FUNDUSZ SPOŁECZNY

ROZWÓJ POTENCJAŁU I OFERTY DYDAKTYCZNEJ POLITECHNIKI WROCŁAWSKIEJ

Wrocław University of Technology

Control in Electrical Power Engineering

Przemysław Janik, Tomasz Sikorski

POWER QUALITY ASSESSMENT

Wrocław 2011

Projekt współfinansowany ze środków Unii Europejskiej w ramach
Europejskiego Funduszu Społecznego

Wrocław University of Technology

Control in Electrical Power Engineering

Przemysław Janik, Tomasz Sikorski

POWER QUALITY ASSESSMENT

Wrocław 2011

Reviewer: Zbigniew Leonowicz

ISBN 978-83-62098-64-4

Published by PRINTPAP Łódź, www.printpap.pl

Content

1. INTRODUCTION 4

2. OVERVIEW OF DISTURBING PHENOMENA AND INDICES 6

2.1. MOTIVATION FOR SYSTEMATICAL APPROACH 6
2.2. VOLTAGE SAG 7
2.3. BRIEF INTERRUPTIONS 8
2.4. VOLTAGE SWELLS 9
2.5. TRANSIENTS 10
2.6. UNBALANCE 10
2.7. HARMONIC DISTORTION 11
2.8. FLICKER 13
2.9. POWER QUALITY STANDARDS 14
2.10. LITERATURE 15

3. RESONANCES 16

3.1. PROBLEM FORMULATION 16
3.2. ASSESSMENT OF SERIES RESONANCE 18
3.3. ASSESSMENT OF PARALLEL RESONANCE 21
3.4. LITERATURE 26

4. ANALOG FILTER DESIGN METHODOLOGY FOR HARMONIC CANCELATION 26

4.1. PROBLEM FORMULATION 26
4.2. HIGHER ORDER HARMONICS ORIGINATING IN NONLINEAR LOADS 28
4.3. CURRENTS DRAWN BY A NON-SINUSOIDAL LOAD, GENERAL CHARACTERISTIC 29
4.4. BASIC DEPENDENCIES IN THE RESONANT CIRCUIT SELECTED FOR THE FILTER 32
4.5. PROPOSED DESIGN FOR EFFICIENT HARMONIC FILTRATION 35
4.6. COMPUTATION OF FILTRATION PARAMETERS 36
4.7. SIMULATION OF NONLINEAR LOAD WORKING WITH A FILTER 39
4.8. LITERATURE 42

5. FOURIER TECHNIQUES FOR SPECTRAL ANALYSIS 42

5.1. DISCRETE TIME FOURIER TRANSFORM DEFINITION 43
5.2. DISCRETE FOURIER TRANSFORM DEFINITION 45
5.3. DISCRETE FOURIER TRANSFORM EXPRESSED USING TRIGONOMETRIC FUNCTIONS 47
5.4. PROPERTIES OF DFT 56
5.5. SHIFTING THEOREM IN DFT 58

5.6. Inverse Discrete Fourier Transform ... 62
5.7. DFT Leakage (Ambiguity) and its minimization ... 62
5.8. Windows types and their properties ... 70
5.9. Resolution of the DFT, filling with zeros, sampling in the frequency domain ... 72
5.10. Literature ... 74

6. SYMMETRICAL COMPONENTS FOR CURRENT AND VOLTAGE UNBALANCE ASSESSMENT ... 75

6.1. Mathematical Background ... 76
6.1.1. Complex transformation parameter a ... 76
6.1.2. Symmetrical components definition ... 77
6.1.3. Symmetrical components of voltage, current, impedance and admittance ... 79
6.1.4. Basic properties of symmetrical components ... 80
6.2. Ohm's low for symmetrical components ... 81
6.3. Kirchhoff's current low and voltage low for symmetrical components ... 83
6.4. Filtering of symmetrical components ... 84
6.4.1. Zero sequence filtering ... 85
6.4.2. Positive and negative sequence components filtering ... 86
6.5. Determination of unbalance with accordance to international standards ... 90
6.5.1. Unbalance factor ... 90
6.5.2. Evaluation according to standards ... 91
6.6. Literature ... 92

7. ADVANCED TOPIC. DETERMINATION OF TRANSIENT PARAMETERS IN WIND ENERGY CONVERSION SYSTEM ... 92

7.1. Motivation and problem formulation ... 92
7.2. Prony metod ... 93
7.3. Nonlinear regression method ... 96
7.4. Wavelet Transform ... 97
7.5. Simulation of induction generator with capacitors ... 99
7.6. Parameters of transients computed using Prony algorithm and Nonlinear Regression ... 100
7.7. Concluding remarks ... 105
7.8. Literature ... 105

8. COMPUTATIONAL APPLICATION OF POWER QUALITY ASSESSMENT: DIPS ... 107

8.1. Methods of voltage magnitude estimation ... 109
8.2. Application of rms trend calculation in Matlab ... 113
8.3. Comparison of the methods ... 119
8.4. Dip duration ... 121
8.5. Phase-angle jump ... 125

8.6. MONITORING MODE IN VOLTAGE DIPS ASSESSMENT 128
8.7. DIP TRANSFER IN POWER SYSTEMS 132
8.8. LITERATURE 137

9. COMPUTATIONAL APPLICATION OF POWER QUALITY ASSESSMENT: HARMONICS 139

9.1. HARMONICS DISTORTION AND FOURIER SERIES PARAMETERIZATION 140
9.2. INVESTIGATED PHENOMENA 143
9.3. "LINEAR" SPECTRUM ESTIMATION USING FFT: 145
9.4. HARMONICS AND SUBDIVISION INTO EVEN AND ODD HARMONICS 148
9.5. GROUPS OF HARMONICS, INTERHARMONIC AND SUHARMONIC 150
9.6. LITERATURE 155

10. ELEMENTS OF POWER QUALITY REPORT 156

10.1. POWER FREQUENCY ASSESSMENT 158
10.2. SUPPLY VOLTAGE VARIATION 159
10.3. FLICKER SEVERITY 160
10.4. VOLTAGE UNBALANCE ASSESSMENT 161
10.5. HARMONICS ASSESSMENT 162
10.6. SUMMARY OF THE REPORT 165
10.7. LITERATURE 165

1. Introduction

Power Quality (PQ) topics are of outmost importance in our world strictly dependent on continuous supply of electrical energy.

The field of Power Quality has no strictly defined borders as continuously more and more topics are being discussed in this area. A brief glance at headings of the international conferences justifies the presumption. *The International Conference on Harmonics and Quality of Power* (ICHQP) and *The International Conference on Renewable Energies and Power Quality* ICREPQ are two good examples reflecting the research activities across continents.

From the technical point of view we have a steady growing number of nonlinear loads, electronic controlled devices saving lamps etc., drawing highly non sinusoidal currents. On the other hand, computers, electronic control systems and protection devices are vulnerable and prone to power quality disturbances. The electrical network may be seen as an interconnection between the sinks and the sources of electrical disturbances. Standards and legal regulations help to find the “golden section” between allowed vulnerability of devices and allowed distortion levels in the electrical network.

The title of the book indicates strictly its purpose. In the vast area of PQ, it should give a student an inside look into the theoretical background of Power Quality assessment. So that reading and understanding of changing standards, procedures and technologies will be smooth and based on relatively solid foundations. It should help the students to focus on PQ problems in every day life of electrical engineer working in the deregulated environment.

After the Introduction, a brief overview of basic disturbing phenomena, their origin, effects and mitigation methods is given in Chapter 2.
In Chapter 3, the reader is given information about a common but dangerous phenomenon of resonances. The conditions for parallel and series resonance are given along with features and possible thread for the electrical components.

Chapter 4 presents an effective approach to an analog filter design helping to reduce harmonics. As the filter uses the idea of resonance, it is a natural consequence of the previous chapter. The theoretical presentation is rounded up with practical implementation and simulated filtration results.

Chapter 5 is a fulfillment or a logical consequence of the previous one. If we want to cancel or filter harmonics we should firstly assess their presence in the electrical grid. Fourier transform is a popular and powerful method in spectral analysis. However, appropriate computation of spectral components requires from the engineer at least basic knowledge of DFT properties and features.

Chapter 6 gives us the look into a three phase system. Previously presented topics can be usefully used for every phase of the three phase system separately, or for all of them together. Symmetrical components and symmetry as a global look at a three phase system are inevitable in the assessment of power quality for the results of non symmetry are disastrous.

Chapter 7 is an example of an advanced approach to signal parameters estimation in a system with a wind generator. The complete process has been shown. Starting with the introduction and motivation through methodology and algorithms up to the discussion of results.

Chapter 8 is dedicated to undervoltage event member, called voltage dips (or sags). A proper classification of this event requires an estimation of voltage magnitude as well as time duration during the dip. This chapter introduces mathematical backgrounds as well as a practical application of algorithms in Matlab environment with comparison and examples. In order to emphasize rules of the dips transfer in the power systems an example of a power system model is presented.

Chapter 9 is dedicated to application of Fast Fourier Transform for spectrum estimation. Selected issues of harmonics, interharmonics and harmonics group are introduced. Demonstration algorithms in Matlab and its results are presented on the basis of real measured signal of dc-arc furnace plant.

The aim of chapter 10 is to present an example of power quality report including the assessment of mentioned crucial parameters. Measurements were done in the main point of the supply of the factory which has an electronic assembly line including robots and power electronics.

2. Overview of disturbing phenomena and indices

The overview of disturbing phenomena starts with a brief, systematized motivation formulation of the interest in power quality, generally. This text is mainly based on [2].

In the context of power quality, a disturbance is a temporary deviation from the steady state of waveform caused by faults of brief duration or by sudden changes in the power system. The disturbances considered by the International Electromagnetic Commission include voltage dips, brief interruptions, voltage increases, impulsive transients and oscillatory transients [2].

Nevertheless, waveform distortions (e.g. harmonics), unbalance, voltage fluctuation and flicker indicate clearly the deterioration of power quality. They are also mentioned in standards, and therefore will be introduced.

2.1. Motivation for systematical approach

Before a detailed presentation of disturbances types is given, there is a need for justification of the systematic approach to Power Quality. The individual topics discussed in this field are rather not new. What is new is the system approach in the engineering, seeking interconnections and dependences between various, seemingly independent phenomena. A global assessment is needed to operate the electrical system safely and reliably. That is why disturbances have been grouped into classes which are simultaneously controlled and checked at various points of the electrical system.

Generally, there are four major reasons for the systematic approach and growing interest in Power Quality [1].

- Load equipment is more sensitive to power quality variations than equipment applied in the past. Many new load devices contain microprocessor based controls and power electronic devices that are sensitive to many types of disturbances.
- The increasing emphasis on overall power system efficiency has resulted in a continued growth in the application of devices such as high-efficiency, adjustable speed motor drives and shunt capacitors for power factor correction to reduce losses. This results in increased harmonic levels on power systems and has many people concerned about the future impact on system capabilities.

- Increased awareness of power quality issues by the end users. Utility customers are becoming better informed about such issues as interruptions, sags, and switching transients and challenge the utilities to improve the quality of power delivered.
- Many things are now interconnected in a network. Integrated processes mean that the failure of any component has much more important consequences.

Interestingly, the equipment installed to increase the productivity is also often the equipment that suffers the most from common power disruptions. And the equipment is sometimes the source of additional power quality problems.

2.2.Voltage sag

Voltage sag (sometimes called a dip) is defined as a sudden reduction of the voltage, ranging between 10% and 90% of the nominal voltage. The duration of a sag is from 0.5 cycle, up to several seconds. An example of a symmetrical voltage sag in a three phase system is shown in Figure 2.1.

Common sources of voltage sags are switching operations in the electrical network, changing transformer taps, changing configuration of the grid, switching heavy loads, especially electrical drives. Faults often affect a wide area causing sags lasting as long as the clearing of the fault. the simplified principle of the phenomenon is shown in Figure 2.2. The severity of a particular sag originating in a fault may be given by a simple formula

$$U_{sag} = \frac{Z_Z}{Z_S + Z_Z} \cdot E \tag{2.1}$$

The effect of voltage dips on equipment depends on both parameters of a sag, its duration and magnitude. Computer manufacturers developed a standard correlating the duration and severity of a sag with electronic equipment immunity, called CBEMA. The possible effect on equipment are extinction of discharge lamps, incorrect operation of control devices, speed variations and stopping of motors, tripping of contactors, computer miss operation [2]. And many more.

There is no simple and cheap protection against voltage sags. In case of small loads uninterrupted power supplies UPS are quite efficient. The use of power conditioners or even rebuilding of the electrical grid to reduce voltage losses on impedances are suggested for greater loads.

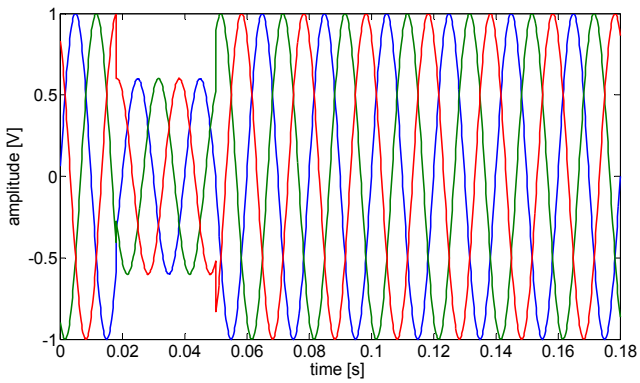

Figure 2.1 Three phase voltage sag, symmetrical case

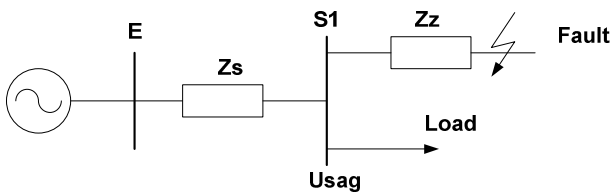

Figure 2.2 Simplified model of a voltage divider representing the proliferation of sags

2.3. Brief Interruptions

No voltage at all may be considered as the most severe sag at all. The effects on equipment is an immediate shut-down and an unexpected stop of operation. Lost data and interrupted industrial processes may lead to huge financial losses.

An example of a three phase voltage interruption is shown in Figure 2.3.

The prime protection procedure against short interruptions is installation of uninterrupted power supplies.

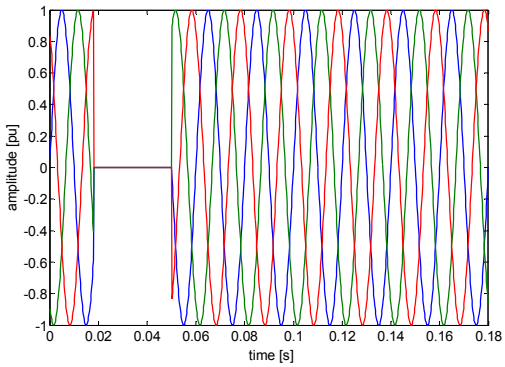

Figure 2.3 Voltage interruption in a three phase system.

2.4.Voltage swells

Voltage swell is the opposite of a sag. A swell is defined as an increase to between 1.1 and 1.8 in pu for durations from 0.5 cycle to several seconds. Swells are also characterized by its magnitude and duration. A three phase case is shown in Figure 2.4. An unsymmetrical voltage swell is often present in un-faulted phases when a single phase fault occurs [2].

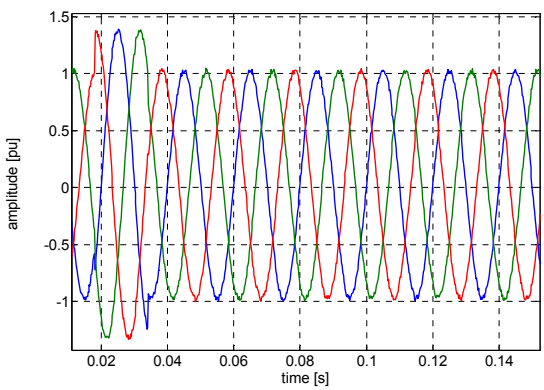

Figure 2.4 Symmetrical voltage swell in a three phase system

Swells can upset electric controls and electric motor dives, which can trip because of their build in protection devices.

A possible solution to the problem is the application of uninterruptible power supplies and conditioners.

2.5.Transients

Voltage disturbances shorter than sags or swells are classified as transients and are caused by sudden changes in the power system. An example of a voltage sag is shown in Figure 2.5.

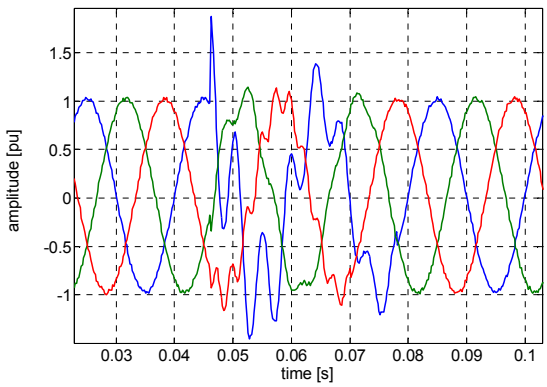

Figure 2.5 Oscillatory transient in a three phase system

According to their duration, transient overvoltages can be divided into switching surge (duration in the range of milliseconds), and impulse spike (duration in the range of microseconds).

Surges are high energy pulses arising from power system switching disturbances, either directly or as a result of resonating circuits associated with switching devices. They also occur during step load changes.

Capacitor switching can cause resonant oscillations leading to an overvoltage some three to four times of the nominal rating, causing tripping or even damaging protective devices and equipment. Electronically based controls for industrial motors are particular susceptible to these transients.

Protection against surges and impulses is normally achieved by surge-diverters and arc-gaps at high voltages and avalanche diodes at low voltages.

Faster transients in nanoseconds due to electrostatic discharges, an important category of EMC, are not normally discussed under power quality.

2.6.Unbalance

Unbalance describes a situation in which either the voltages of a three-phase voltage source are not identical in magnitude or the phase differences between them are not 120 electrical

degrees between them, or both. An example of unbalanced three phase voltages is shown in

.

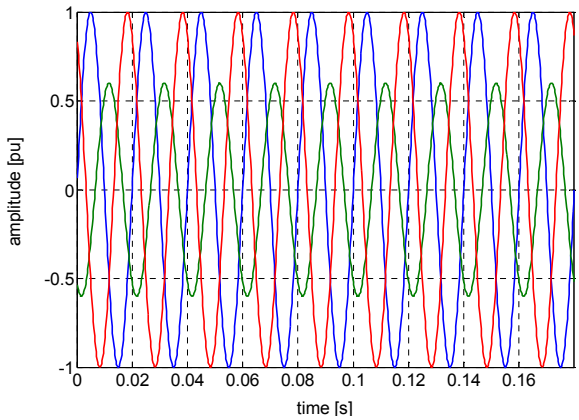

Figure 2.6 Voltage unbalance

The degree of unbalance is usually defined by the proportion of negative and zero sequence components. This subject is discussed extensively in the chapter dedicated to unbalance.

The main causes of unbalance are single phase loads and un-transposed overhead transmission lines.

An electrical machine operating on an unbalanced supply will draw a current with a degree of unbalance several times that of the supply voltage. As a result, the three phase currents may differ considerably and a temperature rise will take place in the machine.

Motors and generators may be fitted with protection to detect extreme unbalance. If the supply unbalance is sufficient, the single phase protection may respond to the unbalanced currents and trip the machine.

2.7.Harmonic distortion

Waveform distortion is generally discussed in terms of harmonics. This is a fast subject for which special books have been dedicated [3]. At this point only a general introduction will be given. Three phase signal distorted by harmonics is shown in Figure 2.7.

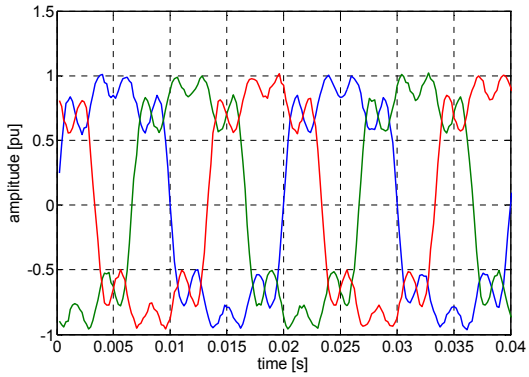

Figure 2.7 Three phase signal distorted by harmonics

Generally, any non-linear load is a source of current harmonics in the electrical system. The harmonic sources can be grouped into three categories according to their origin, size and predictability:

- small and predictable (domestic and residential appliances)
- large and random (arc furnaces, welders)
- large and predictable (static converters, HVDC transmission)

The main detrimental effects of harmonics are:

- maloperation of control devices, signaling systems, protective relays
- extra losses in capacitors, transformers and rotating machines
- additional noise from motors and other apparatus
- telephone interference
- the presence of power factor correction capacitors and cable capacitance is a potential reason for shunt and series resonances resulting in voltage amplification

To keep the harmonic voltage content within the recommended levels the main solutions are:

- the use of high pulse rectification (e.g. in HVDC transmission systems)
- passive filters, either tuned to individual frequencies or of the band pass type.
- active filters and conditioners

2.8.Flicker

Flicker has been described in [4] as:

“the impression of fluctuating luminance or color occurring when the frequency of the variation of the light stimulus lies between a few hertz and the fusion frequency of images. This is a very loose definition considering that “the fusion frequency of images” varies from person to person and depends on many factors.

Fluctuation of the system voltage (more specifically in the r.m.s. value) can cause perceptible (low frequency) light flicker depending on the magnitude and frequency of the variation. Power system engineers call this type of disturbance “voltage flicker” but often it is just shortened to “flicker”.

A simple flicker in a three phase system is shown in Figure 2.8. It represents a simple case of a voltage flicker, when the a.c. voltage is modulated (amplitude modulation) by a sine wave seen as the envelope of the voltage waveform.

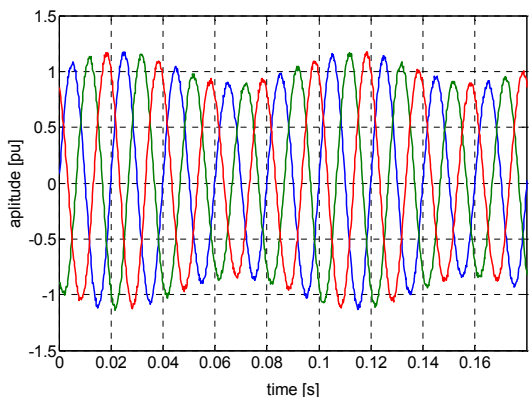

Figure 2.8 Voltage flicker in a three phase system

The general mathematical expression for a flicker is given by

$$v(t)=\left(\alpha_0+\sum_{i=1}^{M}\left\{\alpha_{fi}\sin\left(\beta_{fi}\omega_0 t+\varphi_{fi}\right)\right\}\right)\sin\left(\omega_0 t+\varphi_0\right) \tag{2.2}$$

and can be interpreted as modulation by a sine wave with relatively low frequency.

Non-periodic events can also cause a perceptible light flicker. Any potentially perceptible change in brightness should therefore be termed light flicker, broadening the given definition further by extending the lower frequency limit to non-periodic disturbances.

The main causes of flicker are loads drawing large and highly variable currents. Due to the impedance of the power system (generators, transformers and transmission lines) these

changes produce amplitude modulation of the voltage at the load bus and even at remote busses. Another common source of flicker is the starting of electric motors. Their operation in application that require an irregular torque is problematic. Motor applications range from household appliances up to more powerful appliances such as heat pumps or rolling mills. These flicker sources lead to electric lamp luminance fluctuations by means of amplitude modulation of the supply voltage.

The flickering of electric light causes annoyance to human observers. It reduces the live of electronic devices, incandescent and fluorescent devices, malfunction of phase-locked-loops and loss of synchronism in uninterruptible power supplies, maloperation of electronic controllers and protection devices.

2.9.Power Quality Standards

Te development of standards and guidelines is centered around the following objectives [5]:

- description and characterization of the phenomena
- major sources of power quality problems
- impact on other equipment and on the power system
- mathematical description of the phenomena using indices or statistical analysis to provide a quantitative assessment of its significance
- measurement techniques and guidelines
- emission limits for different types and classes of equipment
- immunity or tolerance level of different types of equipment
- testing methods and procedures for compliance with limits
- mitigation guidelines

The internationally recognized organization for standardization is the International Electrotechnical Commission which is based in Geneva. IEC has defined a series of standards, called Electrotechnical Capability, to deal with power quality issues. This series is published in separate parts according to the following structures.

1. General (IEC 61000-1-x) the general section introduces and provides fundamental principles on EMC issues and describes the various definitions and terminologies used in the standards

2. Environment (IEC 61000-2-x) this part describes and classifies the characteristics of the environment or surroundings where equipotent will be used. It also provides guidelines on compatibility levels for various disturbances.
3. Limits (IEC 61000-3-x) this section defines the maximum levels of disturbances caused by equipment or appliances that can be tolerated within the power system. It also defines the immunity limits or equipment sensitive to EMC disturbances.
4. Testing and Measurement Techniques (IEC 61000-4-x)these provide guidelines on the design of equipment for measuring and monitoring of power quality disturbances. They also outline the equipment.
5. Installations and Mitigation Guidelines (IEC 61000-5-x) this section provides guidelines on the installation techniques to minimize emission and as well as to strengthening immunity against EMC disturbances. It also describes the use of various devices for solving power quality problems.
6. Generic Standards (IEC 61000-6-x) these include the standards specific to certain category of equipment or for certain environments. They contain both emission limits and immunity levels standards

Some of the other organizations who have developed their own standards are CENELEC, UIE, IEEE, ANSI, NEMA. These standards are usually very much application based on or specific to a certain environment.

The standard EN 50160 Voltage Characteristics in Public Distribution Systems is widely used in Europe and directly build-in into commercial power quality metering devices. This standard, or its pats is also included in legal regulations concerned with power quality.

2.10. Literature

[1] R. C. Dugan, M. F. McGranaghan, H. W. Beaty, Electric Power Systems Quality, McGraw-Hill, New York, 1996

[2] J. Arrilaga, N. R. Watson, Power System Quality Assessment, John Wiley and Sons, Chichester, 2000

[3] J. Arrillaga, N. R. Watson, Power System Harmonics, Wiley and Sons, Chichester, 2003

[4] IEEE, Standard Dictionary of Electrical and Electronic Terms, Std.100, IEEE, 1984

[5] J. Arrillaga, D.A. Bradley, P.S. Bodger, Power System Harmonics, John Wiley & Sons, 1985

3. Resonances

Resonances are a common phenomenon in an electrical network. The occurrence of resonance is directly connected with other power quality issues. If there are unexpected harmonics, then the damage to system components may be high due to resonances. On the other hand, the resonance phenomenon is exploited in filtering devices, to short-circuit the unwanted harmonics. That's why the resonance issue coms first. The presentation and the problem formulation is directly based on [3].

3.1. problem formulation

When the voltage applied to an electrical network containing resistance, inductance and capacitance is in phase with the resulting current, the circuit is said to be **resonant.** At resonance, the equivalent network impedance is purely resistive, since the supplied voltage and current are in phase. The power factor of a resonant network is unity [1].

Apart from power quality issues, the phenomenon of the resonance is of a great value in communication engineering. It enables small portions of the communication frequency spectrum to be selected for amplification independently of the remainder.

However, there is also a potential thread inherent in this phenomenon. If a voltage resonance or a current resonance is present in an electrical network, it may be dangerous for system components (damaged insulation, flash over, etc.).

Excess current or voltage may be dangerous for insulation of wires and components. Especially capacitors and transformers insulation is vulnerable to high voltages. Measuring transformers may also be damaged. Currents higher than allowed are responsible for additional mechanical stress put on all current leading elements. There is also additional heat accelerating the aging process of insulation. There is also a risk of saturation in transformers. Electrical apparatus, measuring transformers other devices malfunction can often be led back to unwanted resonances.

Special care is needed during the design process to avoid resonances for normal operation condition at 50 Hz. The situation becomes more complicated if harmonics and

interharmonics are present in current or voltage due to changes of capacitance and inductance along with frequency. That means, if there is a problem with harmonics, the risk of resonances is significantly higher. The common source of harmonics are nonlinear devices of any type, mostly power electronic. Special harmonic filters are designed for them. A slightly more difficult situation results from transient overvoltages and overcurrents. Lightning and capacitor switching are very typical examples. Capacitors are used to provide reactive power to correct the power factor, they are cheap and sufficient, but switching operations are quite frequent.

A wind generator equipped with compensating capacitors, as an example of a system component with variable consumption of reactive power is shown in Figure 3.1 [2]. Due to the variable consumption of reactive power, let us stress it again, the switching operations are frequent. The parameters of oscillatory transient vary with changing wind conditions and system parameters. An example of current time curve is shown in Figure 3.2.

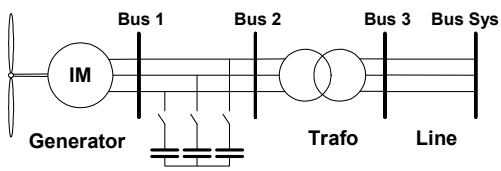

Figure 3.1 Induction generator with compensating capacitors

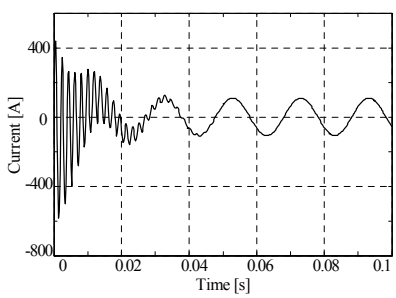

Figure 3.2 Current resulting from capacitor bank switching in wind generator

There is no doubt about the necessity to avoid resonances in electrical networks. The systematic presentation of the phenomenon starts with the computation of conditions for series or parallel resonance. Then, follows the computation of the resonant frequency, determining the maximal voltage or current values.

Basic ideas for series resonance and parallel resonance will be shown below. All voltages and currents are complex, unless otherwise noticed.

3.2.Assessment of series resonance

Figure 3.3 shows a circuit comprising a coil of inductance L, resistance R and capacitance connected in series [3].

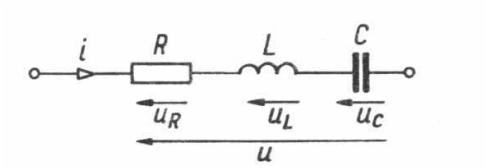

Figure 3.3 R, L, C elements connected in series

The voltage across the series RLC circuit is given by

$$U = U_R + U_L + U_C \tag{3.1}$$

The circuit is at resonance, if $U_L + U_C = 0$, also

$$\left(\omega_0 L - \frac{1}{\omega_0 C}\right) I = 0 \tag{3.2}$$

Thus,

$$\omega = \frac{1}{\sqrt{LC}} \tag{3.3}$$

and the frequency at resonance

$$f = \frac{1}{2\pi\sqrt{LC}} \text{ Hz} \tag{3.4}$$

Figure 3.4 shows how the reactance and inductance and their algebraically added values vary with changing frequency.

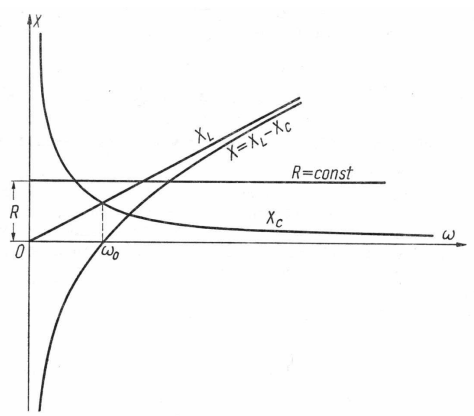

Figure 3.4 Variations of R, X_L, X_R with the frequency

Since (3.2) is fulfilled at resonance, then the impedance $Z = R = \text{constant}$. This is the minimum possible value of impedance and the current reaches its maximum.

At frequencies less than $f_0\ (\omega_0)$, $X_L < X_C$ the circuit is capacitive, at frequencies higher than $f_0\ (\omega_0)$, $X_L > X_C$ the circuit is inductive.

The inductive reactance or capacitive reactance at resonance frequency is called *characteristic impedance* (*wave impedance*) and usually denoted with ρ.

$$\rho = \omega_0 L = \frac{1}{\omega_0 C} = \sqrt{\frac{L}{C}} \tag{3.5}$$

Quality factor or Q-factor [1] in series resonance is the ratio of characteristic impedance to the resistance

$$Q = \frac{\rho}{R} \tag{3.6}$$

Therefore the Q-factor of capacitor and inductive coil at resonance is equal to

$$Q_L = \frac{\omega_0 L}{R} = Q_C = \frac{1}{R\omega_0 C} \tag{3.7}$$

In other words, the Q-factor is a ratio of voltage across reactive element to the voltage across resistance. (3.8)

$$Q = \frac{U_L}{U_R} = \frac{U_C}{U_R} \tag{3.9}$$

Equation (3.9) indicates other name of Q - *circuit magnification factor*.

The Q-factor is defined in general using the energetic approach [4]. Let us multiply the numerator and denominator of (3.9) by $\frac{1}{2} {I_m}^2$

$$Q = \omega_0 \frac{\frac{1}{2} {I_m}^2 L}{\frac{1}{2} {I_m}^2 R} = 2\pi \frac{\frac{1}{2} {I_m}^2 L}{RT \frac{1}{2} {I_m}^2} = 2\pi \frac{W_{L\,\max}}{W_R(T)} \tag{3.10}$$

where $W_{L\,\max}$ is the maximal energy storied in the magnetic field of a coil and $W_R(T)$ energy lost at resistance during one period T. The Q-factor is multiplied by 2π ratio of maximal energy storied in an inductive coil to the energy lost in resistance over one period.

Let us assume that the voltage source frequency feeding RLC branch is variable. If the frequency is ω_0, we say that the circuit is *tuned to resonance*. If the angular frequency ω is

different from ω_0, we say that the circuit is not tuned to resonance that there is a deviation from the resonant frequency.

In the impedances triangle for a RLC branch, the value of $tg(\varphi)$ is equal to the ratio X/L, which characterizes deviation from resonant frequency ξ.

$$\xi = \frac{X}{R} = tg(\varphi) \quad \text{also} \quad \varphi = arctg(\xi) \tag{3.11}$$

Therefore, impedance of RLC branch may be expressed as

$$Ze^{j\varphi} = R\sqrt{1+\xi^2}e^{j\varphi} \tag{3.12}$$

At resonance $\xi = 0$ and Z=R, also

$$\frac{Z}{R} = \sqrt{1+\xi^2}e^{j\varphi} \tag{3.13}$$

Equation (3.11) is presented graphically for three chosen values of resistance: 5,10 and 20 Ohms (Figure 3.5).

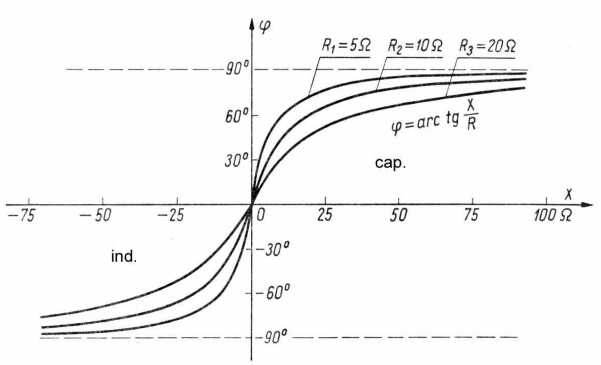

Figure 3.5 Phase angle φ as a function of the deviation from resonant frequency.

Utilising (3.7) we can express the inductance and capacitance as a function of characteristic impedance

$$L = \frac{\rho}{\omega_0} \qquad C = \frac{1}{\omega_0 \rho} \tag{3.14}$$

and substitute the values to the expression for RLC branch reactance we get

$$X = \omega L - \frac{1}{\omega C} = \left(\frac{\omega}{\omega_0} - \frac{\omega_0}{\omega} \right) \rho \tag{3.15}$$

Relative deviation from the resonant frequency δ is given as a ratio of the reactance X and characteristic impedance ρ.

$$\delta = \frac{\omega}{\omega_0} - \frac{\omega_0}{\omega} = \frac{f}{f_0} - \frac{f_0}{f} \tag{3.16}$$

Substituting $k = f / f_0$ we can rewrite (3.16) as

$$\delta = k - \frac{1}{k} \tag{3.17}$$

Deviation from the resonant frequency, relative deviation from the resonant frequency and Q-factor are dependent on each other

$$\xi = Q\delta \tag{3.18}$$

For frequencies near the resonant frequency, it is convenient to apply an approximated expression for δ. The approximated expression is constructed under the assumption that $\omega + \omega_0 \approx 2\omega$, then δ' is given as

$$\delta = \frac{\omega}{\omega_0} - \frac{\omega_0}{\omega} = \frac{\omega^2 - {\omega_0}^2}{\omega\omega_0} = \frac{\omega + \omega_0}{\omega_0} \approx 2\frac{\omega - \omega_0}{\omega_0} = 2(k-1) = \delta' \tag{3.19}$$

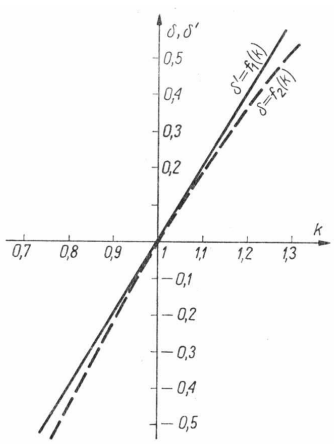

Figure 3.6 relative deviation from the resonant frequency (true and approximated) as a function of relative frequency

3.3.Assessment of parallel resonance

Parallel resonance or current resonance may appear in a circuit with parallel GCL branches (Figure 3.7). For a given complex voltage U .

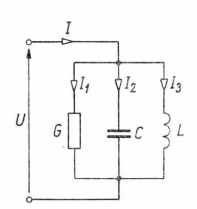

Figure 3.7 Circuit with parallel branches for current resonance

The currents across elements in the branches are given by

$$\left.\begin{aligned} I_R &= GU \\ I_C &= j\omega CU \\ I_L &= -j\frac{1}{\omega L} \end{aligned}\right\} \tag{3.20}$$

The current across capacitor is 90 degrees ahead of the voltage, the current in the coil 90 degrees back after voltage. Both are reactive, only the current across resistance is active. Parallel resonance is characterized by the fact that at the resonance frequency ω_0 currents across a coil and a capacitor are equal in module but opposite in phase (vector sum is zero).

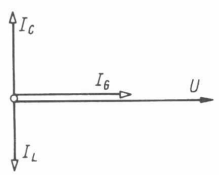

Figure 3.8 Parallel circuit at resonance, reactive current component equal zero

Current resonance (Figure 3.8) is expressed by

$$I_C + I_L = 0 \tag{3.21}$$

also

$$\left(\omega_0 C - \frac{1}{\omega_0 L}\right)U = 0 \tag{3.22}$$

Resonant frequency

$$\omega_0 = \frac{1}{\sqrt{LC}} \tag{3.23}$$

The susceptance of a parallel branch at resonance is zero

$$B = B_C - B_L = \omega_0 C - \frac{1}{\omega_0 L} = 0 \tag{3.24}$$

The voltage across the parallel branch reaches its maximal value in comparison to values reached not at resonance

$$U = \frac{I}{G + j\left(\omega_0 C - \frac{1}{\omega_0 L}\right)} = \frac{1}{G} \tag{3.25}$$

At resonance, the branch is strictly resistive and current is in phase with the voltage.

The characteristic impedance (wave impedance) for a parallel branch is given by

$$\rho = \omega_0 L = \frac{1}{\omega_0 C} = \sqrt{\frac{L}{C}} \tag{3.26}$$

The Q-factor for a parallel branch is defined similarly as for a series circuit and given by

$$Q = \omega_0 \frac{\frac{1}{2} C |U_m|^2}{GU^2} = R\omega_0 C = \frac{R}{\rho} \tag{3.27}$$

but the expression is different from (3.6). Both equation ((3.6) and (3.27)) are given for a particular circuit and can not be generalized.

Deviation from resonant frequency in a parallel circuit is given by

$$\xi = -\frac{B}{G} \tag{3.28}$$

Admittance as a function of deviation from resonant frequency

$$Y = |Y| e^{-j\varphi} = G\sqrt{1+\xi^2} e^{-j\varphi} \tag{3.29}$$

At resonance we have $\varphi_0 = 0,\ Y_0 = |Y_0| = G$, therefore the relative admittance and impedance have the form

$$\left.\begin{aligned} \frac{|Y|}{|Y_0|} &= \sqrt{1+\xi^2} \\ \frac{|Z|}{|Z_0|} &= \frac{1}{\sqrt{1+\xi^2}} \end{aligned}\right\} \tag{3.30}$$

Assuming changing frequency ω and constant absolute value of current $|I|$ the Ohm's law for absolute values

$$|U| = |Z||I| \tag{3.31}$$

Therefore, the characteristic in Figure 3.9 shows the changes of $|Z|/|Z_0|$ as a function of the deviation from resonant frequency which is equal to the curve showing $|U|/|U_0|$.

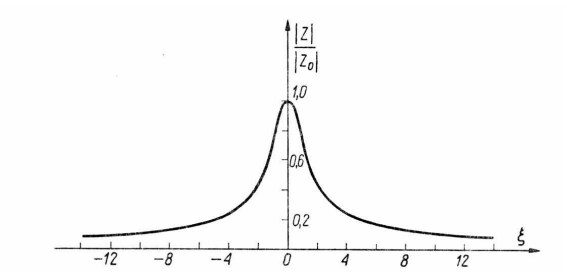

Figure 3.9 Absolute value of relative impedance as a function of deviation from resonant frequency

Accompanying the characteristic of absolute value of relative impedance the characteristic of an admittance phase angle is given in Figure 3.10. It has the form of the function arctg multiplied by minus one.

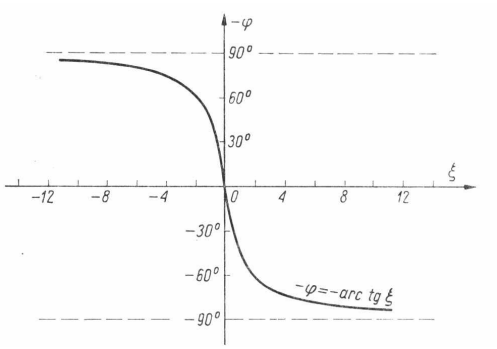

Figure 3.10 Admittance phase angle in parallel GLC branch

According to the definition of characteristic impedance, the values of L and C may be expressed as

$$L = \frac{\rho}{\omega_0}, \quad C = \frac{1}{\omega_0} \tag{3.32}$$

and the susceptance may be expressed as a function of characteristic impedance

$$B = \omega C - \frac{1}{\omega L} = \left(\frac{\omega}{\omega_0} - \frac{\omega_0}{\omega} \right) \frac{1}{\rho} \tag{3.33}$$

Similarly as for parallel branch the relative deviation from resonant frequency

$$\delta = \frac{\omega}{\omega_0} - \frac{\omega_0}{\omega} = \frac{f}{f_0} - \frac{f_0}{f} \tag{3.34}$$

and

$$\xi = Q\delta \tag{3.35}$$

A quite interesting and unusual situation may be present in a parallel circuit with two branches RL and RC (Figure 3.11). Currents at resonant frequency are shown in Figure 3.12 where the compensation of reactive currents takes place.

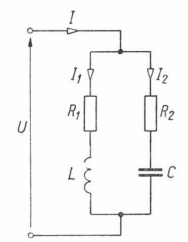

Figure 3.11 Circuit with parallel braches RL and RC

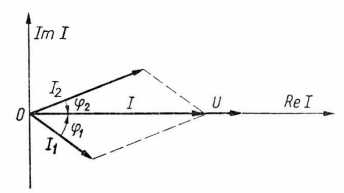

Figure 3.12 Currents in a parallel RL and RC circuit at resonance

The compensation condition is given by

$$|I_1|\sin\varphi_1 + |I_2|\sin\varphi_2 = 0 \tag{3.36}$$

also

$$B_1 + B_2 = 0 = -\frac{X_1}{|Z_1|^2} - \frac{X_2}{|Z_2|^2} \tag{3.37}$$

Applying (3.37) to the circuit in Figure 3.11 we obtain

$$-\frac{\omega L}{R_1^2 + \omega^2 L^2} + \frac{\dfrac{1}{\omega C}}{R_2^2 + \dfrac{1}{\omega^2 C^2}} = 0 \tag{3.38}$$

rewriting this we get

$$\omega^2 L\left(R_2^2 - \frac{L}{C}\right) = \frac{1}{C}\left(R_1^2 - \frac{L}{C}\right) \tag{3.39}$$

where L/C is equal to the squared value of characteristic impedance.

If the resistances of both branches are equal to characteristic impedance

$$R_1 = R_2 = \sqrt{\frac{L}{C}} \tag{3.40}$$

then by every frequency the resonance of currents appears. This is a rare example of a frequency **insensive** circuit. In this particular case, the circuit impedance is

$$Z = \frac{\left(\sqrt{\frac{L}{C}} + j\omega L\right)\left(\sqrt{\frac{L}{C}} - j\frac{1}{\omega C}\right)}{\sqrt{\frac{L}{C}} + j\omega L + \sqrt{\frac{L}{C}} - j\frac{1}{\omega C}} = \sqrt{\frac{L}{C}} \tag{3.41}$$

also the impedance is purely resistive and equal to the characteristic impedance.

For two different resistances the resonant frequency is given as

$$\omega_0' = \frac{1}{\sqrt{\frac{L}{C}}}\sqrt{\frac{\frac{L}{C} - R_1^2}{\frac{L}{C} - R_2^2}} \tag{3.42}$$

If the student is interested in the analysis of more complicated cases it is strongly advisable to refer to [3].

3.4. Literature

[1] John Bird, "Electrical Circuit Theory and Technology", Elsevier, Linacre House, Jordan Hill, Oxford OX2 8DP, UK, 2007, pp. 349-368

[2] Tadeusz Łobos, Jacek Rezmer, Przemysław Janik, Zbigniew Wacławek, "Prony and nonlinear regression methods used for determination of transient parameters in wind energy conversion system", IEEE Lausanne PowerTech, Switzerland, 1-5 July 2007, 6 pages

[3] Tadeusz Cholewicki, "Elektrotechnika Teoretyczna", WNT, Warszawa 1973 pp. 391-422

[4] Stanisław Bolkowski, „Teoria obwodów elektrycznych", WNT, Warszawa, 1995 pp. 150-168

4. Analog filter design methodology for harmonic cancelation

4.1.Problem formulation

One of the various sources of harmonics are widespread lightening systems. Modern lighting systems - street lighting, interior lighting, illumination of buildings must meet multi-criteria

demands imposed by standards and users. One of the demands is reduction of harmonics and interharmonics and guaranteeing good power quality.

Traditional and compact fluorescent lamps, powered via a stabilizing-ignition system, sodium and mercury discharge lamps, light sources powered via power converters contribute significantly to improving the lighting quality and reducing energy costs. Unfortunately, the common feature of all these devices is the non-linearity [1]. The disadvantageous feature is strengthened by other nonlinear devices powered from the same pcc .

Main feature of the nonlinear load is strongly non-sinusoidal current drawn from the grid. This current causes non-sinusoidal voltage drops on transformers' impedances and power lines. It distorts the voltage at pcc, to which other users are connected. Nonlinear loads are the source of power quality deterioration [2], [3].

Non-sinusoidal voltages and currents cause technical problems and obstruct the function of network components (e.g. e automation and protection units), additionally negatively influence other loads [4].

Reduction of harmonics in distribution systems is forced as a result of technical reasoning. Also legal regulations imposed on distribution companies and manufacturers of electrical equipment determine acceptable levels of voltage and current distortion [5], [6], [7].

There is a need for a simple and effective way of reducing the content of harmonics and interharmonics. Analog filters [8] are in use, but a detailed and tedious design process for every application side is required. This article presents the theoretical basis for an efficient filter design, together with sample calculations and simulations carried out for selected characteristic harmonics. The aim of the authors was to deliver an accurate and easy tool do design filters distinguishing selected harmonics and interharmonics. Therefore, the implementation of filters may be very precise and effective. Without detailed calculation for each installation side, application of "average" filter is not advisable.

4.2.Higher order Harmonics originating in nonlinear loads

Nonlinear lighting circuits draw periodical, non-sinusoidal currents *i*. Generally, periodic current can be expressed as the sum of sine waves, forming a Fourier series [8]

$$i_0(t) = I_{m1}\,\boldsymbol{sin}(\omega_0 t + \psi_1) + \sum_{k>1}^{\infty} I_{mk}\,\boldsymbol{sin}(\omega_k t + \psi_k) \tag{4.1}$$

where Imk means the amplitude of the k-th harmonic component, ωk is angular velocity and ψk initial phase shows a signal distorted by 5,7,9 and 11 harmonics.

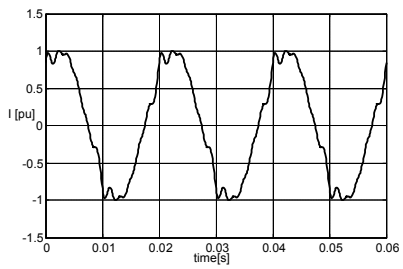

Figure 4.1 Distorted current signal

Harmonics have a direct impact on cables, especially neutral, and transformers. Integer multiples of third harmonic add up in the neutral. Current in which may be, in an extreme case, up to three times higher than in the phase wire. The presence of higher harmonics in the current causes additional heating of cables, therefore, it is dangerous for the insulation. The presence of higher harmonics in voltage increases the current drawn by the capacitors, since the capacitor impedance decreases with increasing frequency.

The magnetic flux in the transformer originating from the third current harmonic is closed outside the core, resulting in the formation of eddy currents in other parts of the transformer [9]. Additional energy losses heat up the transformer interior, so accelerate the aging process of isolation [2].

Higher harmonics also have an adverse impact on the protection [4], in particular the operation of differential-current protection. Harmonics cause also false measuring of electricity meters. They are dangerous for the insulation of cables and compensating capacitor banks, causing heating and damage to insulation. Harmonics cause resonances which are difficult to predict and result in damage to measuring transformers [3].

Higher voltage harmonics are especially dangerous for drives [2]. They generate additional heat loss together with fluctuating value of torque on the shaft.

4.3. Currents drawn by a non-sinusoidal load, general characteristic

Consider a system consisting of a non-linear receiver, connected to the grid (Figure 4.2, left), which in simple terms can be represented in terms of the actual source of sinusoidal voltage (Figure 4.2, right).

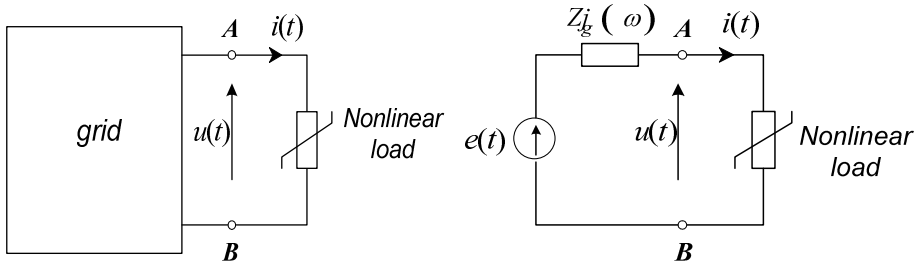

Figure 4.2 non-linear load connected to the grid (l), representation of the network with voltage source (r)

We limit the discussion to steady state. Then, even assuming sinusoidal voltage, the load draws deformed, nonlinear current, containing higher harmonics. Due to the voltage drop across the impedance Zg (Fig. 2), the load will be fed by non-sinusoidal voltage anyway.

The complete elimination of higher harmonics from the currents and voltages waveforms is not possible. We can only minimize the distortion, separating the distortion sources from the grid. Distorted waveforms will be “closed” in a certain “loop”, and load is powered by the fundamental harmonic only. Separators are subsystems with appropriately selected frequency characteristics, such as resonant circuits or filters.

Supposing, that a non-linear load drew the current given by (4.1). Actually, other harmonics may be present due to preexisting voltage distortion. An effective way to determine harmonic (interharmonic) content in the current is direct measurement of the spectrum.

Starting from the compensating theorem [8],[10] and (4.1) we can replace the load by a battery of current sources connected in parallel, each corresponding to the specific harmonic current (Figure 4.3).

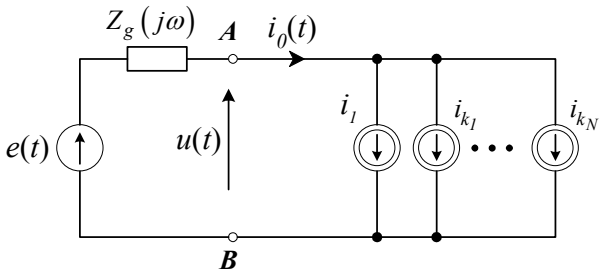

Figure 4.3 Load represented as a battery of current sources

If we place ideal serial resonant branches between the source and the load (Figure 4.4), tuned respectively to each of the higher harmonics, the currents of those frequencies will be completely "separated" from the grid, and the current drawn from the system will contain only the component of fundamental frequency

$$i'(t) = I'_{m1}\,\boldsymbol{sin}\left(\omega_0 t + \psi'_1\right) \tag{4.2}$$

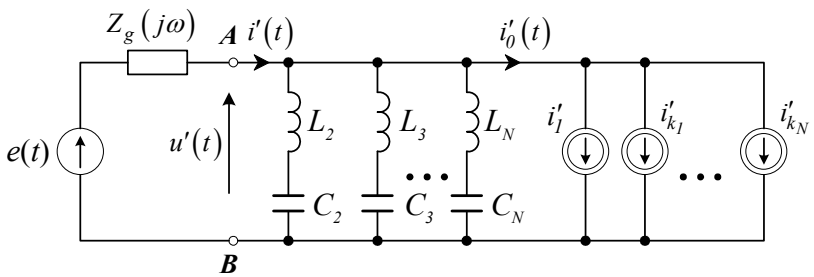

Figure 4.4 Load with ideal resonant branches

However, application of resonant circuits with a very high quality factor is dangerous due to the possibility of significant over-voltages or over-currents. Therefore, instead of ideal branches, circuits in which there is a possibility of regulating the quality factor, are in use. We can modify the circuit in Figure 4.4 by adding a resistor in parallel to the inductance (Figure 4.5). The quality factor can be changed varying the resistance.

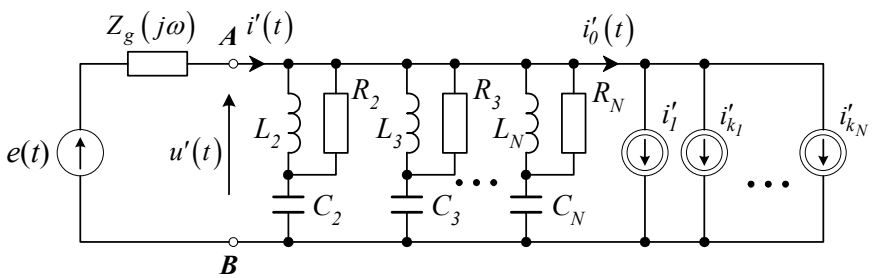

Figure 4.5 Load with resonant branches including resistor

To make a bit more in-depth analysis of the system in Figure 4.5, suppose that this circuit, except the load is a linear circuit, for which the principle of superposition applies. On this basis, the circuit can be studied individually for each harmonic. An example of such a system for the k-th harmonic is shown in Figure 4.6.

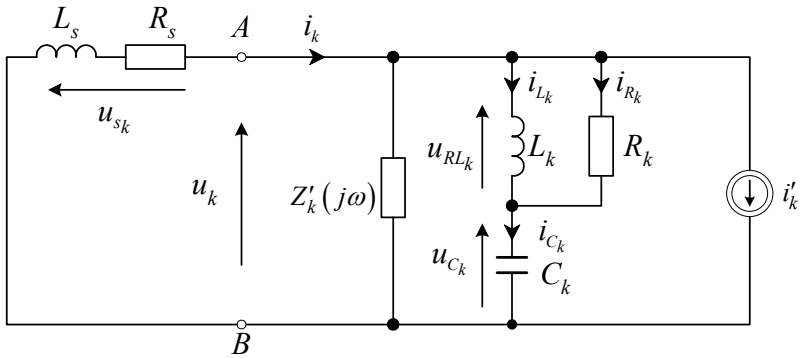

Figure 4.6 Circuit for the k-th harmonic reduction

Assigning the impedance of the k-th resonance circuit by $Z_k(j\omega_k)$ and a summary of all other impedances for the rest of harmonics by $Z'_k(j\omega_k)$ we can define the current of the k-th harmonic as

$$\underline{I}_k = \frac{Z_k(j\omega_k)//Z'_k(j\omega_k)}{Z_k(j\omega_k)//Z'_k(j\omega_k)+Z_s(j\omega_k)}\underline{I}'_k \tag{4.3}$$

where

$$Z_k(j\omega_k)//Z'_k(j\omega_k) = \frac{Z_k(j\omega_k)Z'_k(j\omega_k)}{Z_k(j\omega_k)+Z'_k(j\omega_k)} \tag{4.4}$$

If we select the impedances of resonance circuit in such a way that

$$\left|Z_k(j\omega_k)\right| \square \left|Z'_k(j\omega_k)\right| \tag{4.5}$$

then, the complex value of the k-th current harmonic is given by

$$\underline{I}_k \approx \frac{Z_k(j\omega_k)}{Z_k(j\omega_k)+Z_s(j\omega_k)}\underline{I}'_k \tag{4.6}$$

We can therefore conclude that for absolute values of impedances Zk(jωk) small enough at resonance frequencies, then the harmonic content in current and supply voltage u(t), will be significantly reduced, in comparison to the circuit in Fig. 3. A brief description of the basic

concepts necessary to analyze resonant circuits is given the special respect to the design method presented here.

4.4. Basic dependencies in the resonant circuit selected for the filter

The basic feature describing a resonant circuits is its impedance, defined as a complex function of a real input variable, mostly frequency. Using the impedance function we can compute important parameters - resonance frequency, impedance at resonance, bandwidth. Let us consider a circuit shown in Figure 4.7.

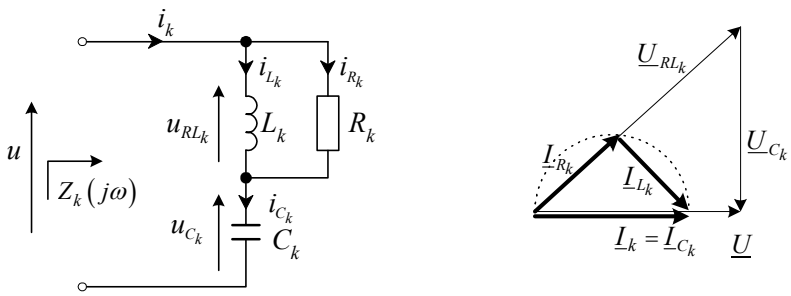

Figure 4.7 Resonance branch and corresponding vector diagram at phase resonance

Assuming that the vectors in Figure 4.7 represent sinusoidal functions with the pulse ω, the complex impedance is defined as the ratio of complex voltage to the complex current value

$$Z_k(j\omega) = \frac{\underline{U}}{\underline{I}_k} = \frac{R_k j\omega L_k}{R_k + j\omega L_k} + \frac{1}{j\omega C_k} = \frac{R_k \omega^2 L_k^2}{R_k^2 + \omega^2 L_k^2} + j\left[\frac{R_k^2 \omega L_k}{R_k^2 + \omega^2 L_k^2} - \frac{1}{\omega C_k}\right] \quad (4.7)$$

Hence, considering the phase resonance condition

$$\boldsymbol{Im}\, Z_k(j\omega) = \frac{R_k^2 \omega L_k}{R_k^2 + \omega^2 L_k^2} - \frac{1}{\omega C_k} = 0 \quad (4.8)$$

We compute the frequency f (angular frequency ω) at resonance

$$\omega_k = \frac{1}{\sqrt{L_k C_k - \left(\frac{L_k}{R_k}\right)^2}}, \qquad f_k = \frac{1}{2\pi\sqrt{L_k C_k - \left(\frac{L_k}{R_k}\right)^2}} \quad (4.9)$$

using the computed value of ω_k we can compute the impedance at resonance

$$\omega = \omega_k \quad \Rightarrow \quad Z_k(j\omega_k) = Z_{k0} = \frac{R_k \omega_k^2 L_k^2}{R_k^2 + \omega_k^2 L_k^2} = \frac{R_k \frac{1}{L_k C_k - \left(\frac{L_k}{R_k}\right)^2} L_k^2}{R_k^2 + \frac{1}{L_k C_k - \left(\frac{L_k}{R_k}\right)^2} L_k^2} = \frac{L_k}{R_k C_k} \quad (4.10)$$

Quality factor Q is an important feature characterizing a resonant circuit. It is defined as a ratio of the maximal energy of the electromagnetic field and energy radiated as heat at resonance during one period [8].

$$Q = 2\pi \frac{W_{max}}{T_0 P_0} \tag{4.11}$$

Where W_{max} - maximal energy of the electromagnetic field, P0 – average power radiated during one period, T_0 – period of the waveform under consideration. For the circuit in Figure 4.7 the expression for the quality factor is given by

$$Q_k = \frac{\frac{1}{\omega_k C_k}}{Z_{k0}} = \frac{R_k}{\omega_k L_k} = R_k \sqrt{\frac{C_k}{L_k}} \tag{4.12}$$

The quality factor is followed by another useful parameter – transmission bandwidth. Transforming ((4.7)) into ((4.13)) we obtain corresponding plot of the impedance absolute value near the resonant frequency (Figure 4.8)

$$\left| Z_k(j\omega) \right| = \sqrt{\frac{R_k^2 \left(1 - L_k C_k \omega^2\right)^2 + \left(\omega L_k\right)^2}{\left(\omega C_k\right)^2 \left[R_k^2 + \left(\omega L_k{}^2\right)\right]}} \tag{4.13}$$

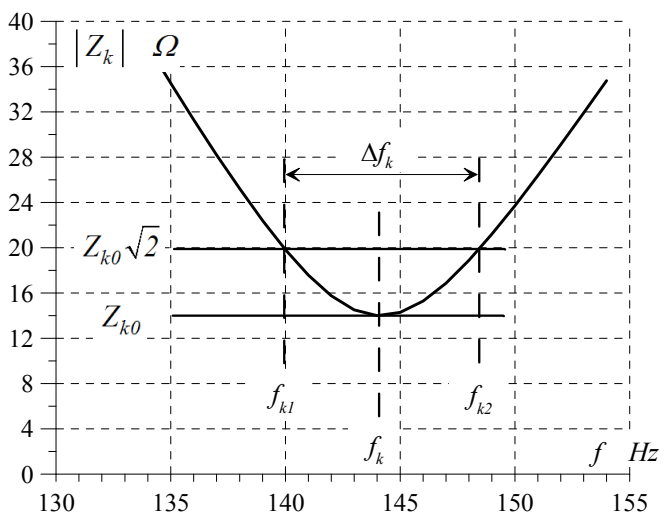

Figure 4.8 Computation of the transmission bandwidth

We observe (Figure 4.8) that the transmission bandwidth is given as the difference of frequencies f_{k1} and f_{k2} for which the impedance absolute value is $\sqrt{2}$ higher than at resonance (power reduced by half).

Exact expression for transmission bandwidth can be given only for relatively simple circuits. In the presented case we apply approximated approach describing the impedance as a function of fractional deviation from the resonant frequency

$$x = \frac{\omega}{\omega_k} = \frac{f}{f_k} \tag{4.14}$$

Putting (4.14) into (4.7) and using (4.9), (4.10) and (4.12) we get a new expression for the impedance

$$Z_k(x) = \frac{Q_k^2 Z_{k0}}{Q_k^2 + x^2 - 1}\left[x^2 + j\frac{\left(Q_k^2 - 1\right)^{\frac{3}{2}}}{Q_k^2 x}\left(x^2 - 1\right)\right] \tag{4.15}$$

Usually, Q factor is significantly higher than 1. Assuming analysis around resonance frequency, we can say that

$$\left.\begin{array}{l} Q_k \gg 1 \\ x \approx 1 \end{array}\right\} \tag{4.16}$$

then

$$Z_k(x) \cong Z_{k0}\left[1 + j2Q_k\left(x - 1\right)\right] \tag{4.17}$$

and

$$\left|Z_k(x)\right|^2 \cong Z_{k0}^2\left[1 + 4Q_k^2\left(x - 1\right)^2\right] \tag{4.18}$$

defining

$$x_1 = \frac{f_{k1}}{f_k}, \quad x_2 = \frac{f_{k2}}{f_k} \tag{4.19}$$

we obtain

$$1 + 4Q_k^2\left(x_{1,2} - 1\right)^2 = 2 \tag{4.20}$$

therefore

$$x_{1,2} = 1 \mp \frac{1}{2Q_k} \tag{4.21}$$

Finally, the bandwidth is

$$\Delta f_k = f_{k2} - f_{k1} = \left(x_2 - x_1\right) f_k = \frac{1}{Q_k} f_k \tag{4.22}$$

In (4.23) we recognize a plain relationship between Q factor and bandwidth. Quality factor Q may be determined using the resonance characteristic

$$Q_k = \frac{f_k}{\Delta f_k} \tag{4.23}$$

The influence of various Q factor values obtained by (4.24) on the shape of the resonance curve is shown in Figure 4.9, where $Z_{k0} = 10\ \Omega, Q_k = 5, 10, 20, 50$.

$$\left|Z_k(x)\right| = \frac{Q_k^2 Z_{k0}}{Q_k^2 + x^2 - 1}\sqrt{x^4 + \frac{\left(Q_k^2 - 1\right)^3}{Q_k^4 x^2}\left(x^2 - 1\right)^2} \tag{4.24}$$

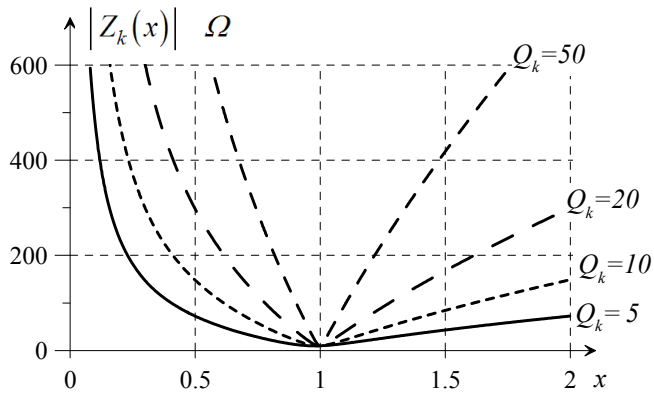

Figure 4.9 Impedance vs. Q factor

Unfortunately, there is a discrepancy between the minimum of impedance and resonance frequency. In practice, it may have a negative impact on filtering accuracy. Therefore, it is advisable to apply a corrective value given by (4.25). It was derived using the small parameter method.

$$f_{k0} \cong f_k\sqrt{1 - \frac{1}{Q_k^2} + \frac{1}{2Q_k^4}} \tag{4.25}$$

4.5. Proposed design for efficient harmonic filtration

Figure 4.10 shows a simplified model of a filter for arbitrary selected harmonics or interharmonics. The idea may be expanded on every frequency, not only an integer multiply of fundamental

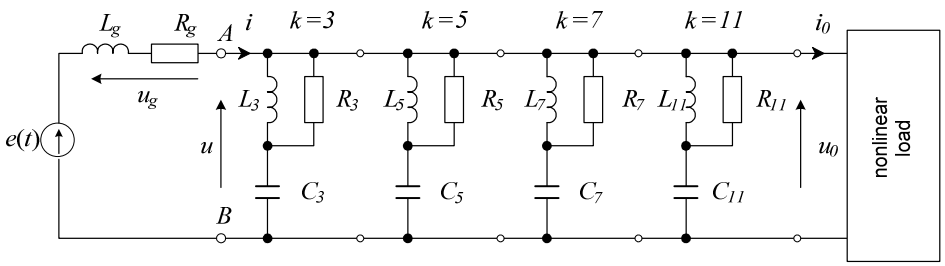

Figure 4.10 Filter for selected harmonics

Using the method given above, the set of expression enabling fast and accurate determination of RLC parameters will be presented.

Usually, there are required values for resonance frequency fk, impedance at resonance Zk0, and Q factor (or bandwidth Δfk). For Q factor smaller than 10, it is recommended to apply the correction given by (4.25). Then, fk is given by

$$f_k \cong \frac{f_{k0}}{\sqrt{1-\frac{1}{Q_k^2}+\frac{1}{2Q_k^4}}} \tag{4.26}$$

From (4.10) and (4.12) we get

$$R_k = Q_k^2 Z_{k0} \tag{4.27}$$

Then we compute the wave impedance ρ

$$\rho^2 = \frac{L_k}{C_k} = \frac{R_k^2}{Q_k^2} = Q_k^2 Z_{k0}^2 \tag{4.28}$$

From(4.28) and (4.9) we obtain

$$L_k = \frac{1}{2\pi f_k}\frac{Q_k^2}{\sqrt{Q_k^2-1}} Z_{k0} \tag{4.29}$$

and

$$C_k = \frac{L_k}{\rho_k^2} = \frac{L_k}{Q_k^2 Z_{k0}^2} = \frac{1}{2\pi f_k}\frac{1}{\sqrt{Q_k^2-1}}\frac{1}{Z_{k0}} \tag{4.30}$$

4.6.Computation of filtration parameters

Mathematical expressions from previous chapters were used in realization of a four section filter for a priori chosen harmonics

$$\begin{aligned} f_{03} &= 150\,Hz, \quad f_{05} = 250\,Hz, \\ f_{07} &= 350\,Hz, \quad f_{11} = 550\,Hz \end{aligned} \tag{4.31}$$

The absolute value of impedance for each resonance frequency can be chosen independently. Equal value was assumed for every harmonics in order to simplify the presentation

$$Z_{03} = Z_{05} = Z_{07} = Z_{011} = 14\ \Omega \tag{4.32}$$

Similarly, the Q factor for every component filter was equalized. Four different cases are summarized in Table 4-1.

Table 4-1 Various values of the Q factor

Case No.	1	2	3	4
$Q_3 = Q_5 = Q_7 = Q_{11}$	5	10	20	50

Tables show the RLC and f values for Q factors from Table 4-1.

Table 4-2 RLC values for the case 1, Q=5

	k = 3	*k = 5*	*k = 7*	*k = 11*
R	350Ω	350Ω	350Ω	350Ω
L	0.074H	0.044H	0.032H	0.020H
C	15.16μF	9.10μF	6.65μF	4.135μF
f	153.03Hz	255.05Hz	357.07Hz	561.11Hz

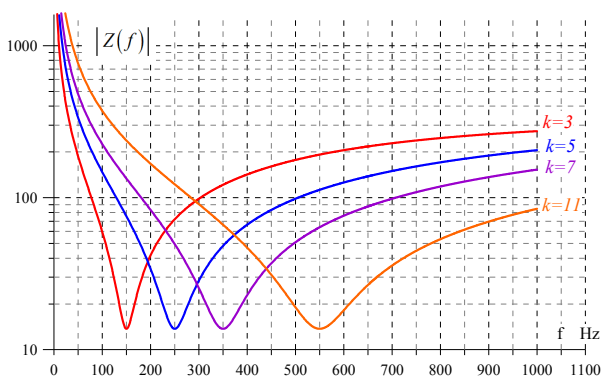

Figure 4.11 Absolute value of impedance for Q=5

Table 4-3 RLC values for the case 1, Q=10

	k = 3	*k = 5*	*k = 7*	*k = 11*
R	1400Ω	1400Ω	1400Ω	1400Ω
L	0.148H	0.89H	0.637H	0.040H
C	7.579μF	4.547μF	3.248μF	2.067μF
f	150.75Hz	251.25Hz	351.75Hz	552.76Hz

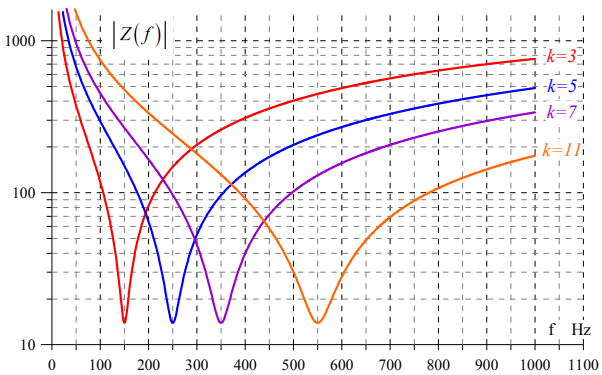

Figure 4.12 Absolute value of impedance for Q=10

Table 4-4 RLC values for the case 1, Q=20

	k = 3	*k = 5*	*k = 7*	*k = 11*
R	1400Ω	1400Ω	1400Ω	1400Ω
L	0.148H	0.89H	0.637H	0.040H
C	7.579μF	4.547μF	3.248μF	2.067μF
f	150.75Hz	251.25Hz	351.75Hz	552.76Hz

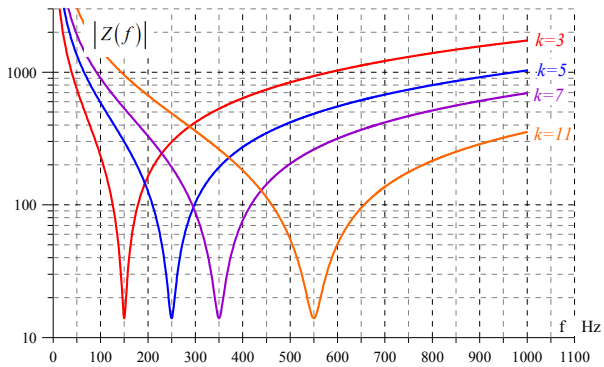

Figure 4.13 Absolute value of impedance for Q=20

Table 4-5 RLC values for the case 1, Q=50

	k = 3	*k = 5*	*k = 7*	*k = 11*
R	35kΩ	35kΩ	35kΩ	35kΩ
L	0.743H	0.446H	0.318H	0.203H
C	1.516μF	0.909μF	0.650μF	0.413μF
f	150.03Hz	250.05Hz	350.07Hz	550.11Hz

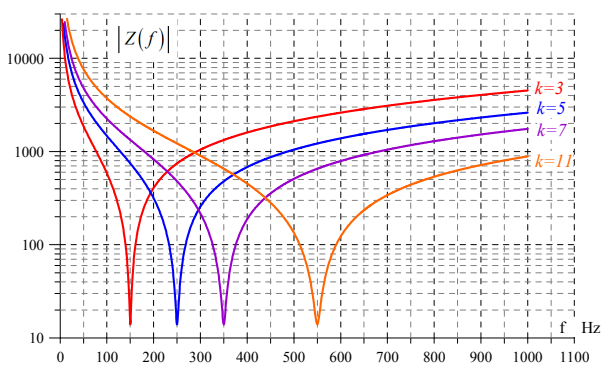

Figure 4.14 Absolute value of impedance for Q=50

4.7. Simulation of nonlinear load working with a filter

Simulation is an effective way to test the presented approach to filter design. The filter was implemented in Power System Bolockset [11], a part of Matlab [12] and shown in Figure 4.15.

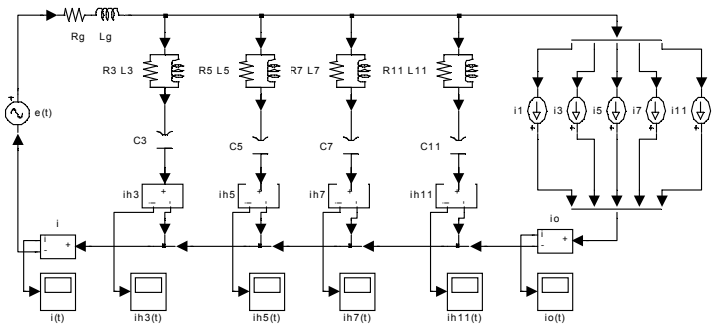

Figure 4.15 Simulated one phase system

To show clearly the filtration effect, the presence of 3, 5, 7, 9, 11 current harmonic was assumed. Every harmonic with an amplitude of 20% of the fundamental. Due to a significant difference between the impedance of the network Zg and the impedance Zf of the filter (50 to 14) the effect of filtering is very clear (Fig. 15). The module of impedance Zf should be selected depending on the impedance of the network, the expected effect of filtration and maximum overcurrent and overvoltage in the filter.

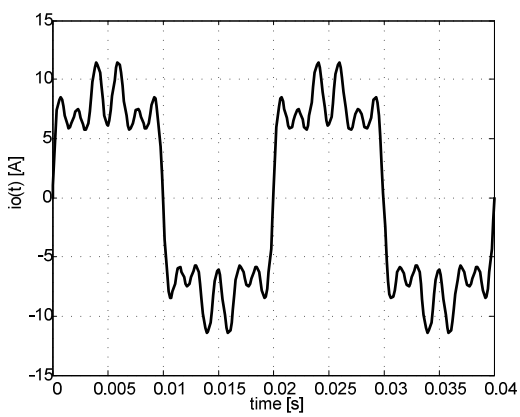

Figure 4.16 Current drawn by nonlinear load

8.3.Comparison of the methods

The comparison of the methods used in process of the rms calculation can be performed on the basis of dynamism of obtained characteristic and computational power and time consumed for calculation. Fig. 8.8 indicates the “peak value” method as a rough estimation of rms changes. This method is the fastest for calculation. The algorithm based on classical rms calculation is comparable with “fundamental component”, however a classical operation does not involve frequency domain calculation and thereby is more attractive in the point of the fast practical application.

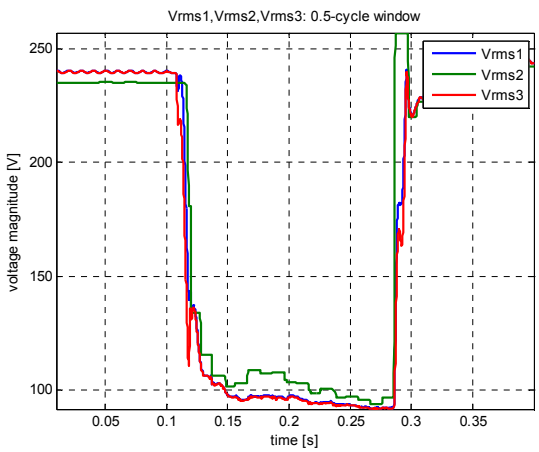

Fig. 8.8. Comparison of the “rms voltage” method (Vrms1), “peak-voltage” method (Vrms2) and “fundamental component” method (Vrms3) for given half-cycle window

The window width, usually defined as a number of cycles of fundamental component, has a crucial meaning for dynamism of rms characteristic, no matter what kind of method is applied. Fig. 8.9,Fig. 8.10,Fig. 8.11 depict a common effect of smearing and reduction of the dynamism of the characteristic when windows longer than one period of fundamental component is applied. Thus, according to the standards, a recommended base of the algorithm is half or one-period of fundamental component.

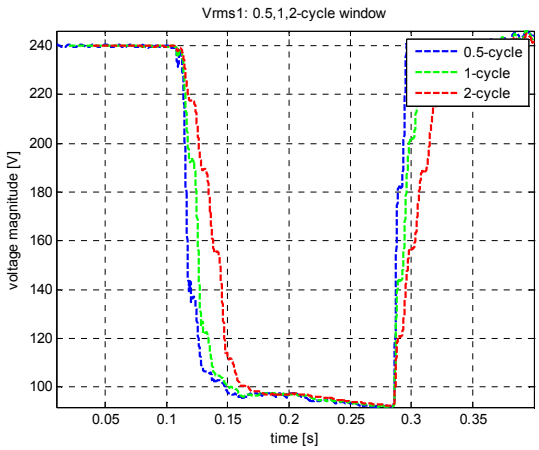

Fig. 8.9. Influence of the window width on “rms voltage” method

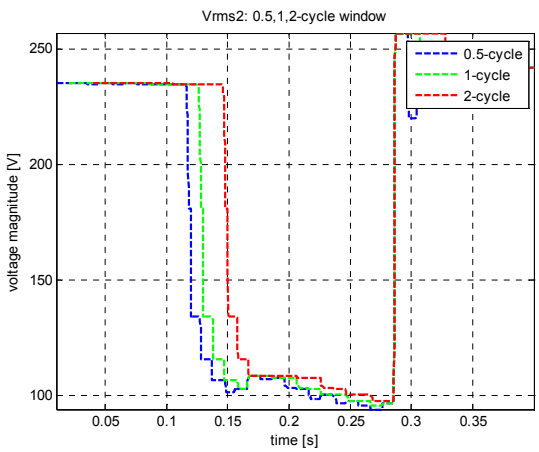

Fig. 8.10. Influence of the window width on “peak voltage” method

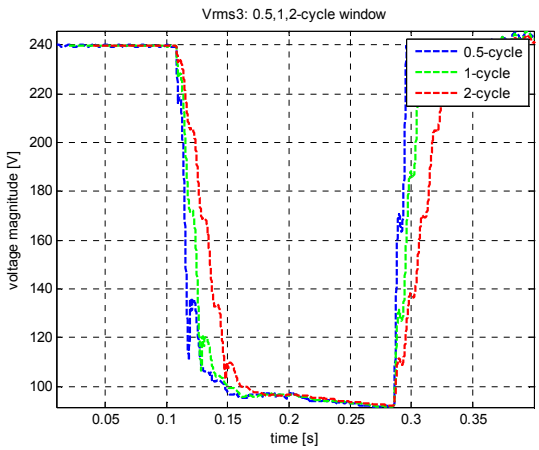

Fig. 8.11. Influence of the window width on “fundamental component” method

8.4.Dip duration

Previous section was concentrated on voltage magnitude estimation during the event. The dip duration is strongly associated with the magnitude variation as a time interval when voltage magnitude is below a given threshold. Referring to the Standards, the threshold initiating dip recognition is 90% of a reference value. Having the detailed information about the recorded phenomena, its origin and voltage condition, we can select nominal value as the reference. However, there are the opinions that allow adapting measured voltage in steady state, before the event, as a reference value. From practical point of view suggested approach uses nominal voltage as reference value in order to set up the threshold.

An example of dip duration identification on the basis of one-cycle “rms voltage” algorithm is shown in Fig. 8.12. The reference value is the nominal voltage in per unit value and the reshold is setup on 90%.

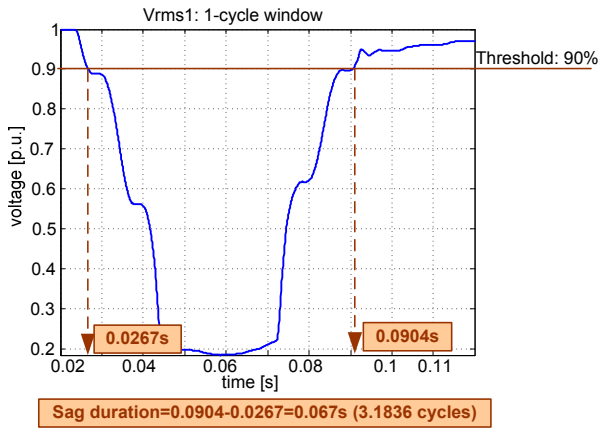

Fig. 8.12. Voltage dip duration identification

Again it must be emphasised that we stay in the high quality mode calculation. It means that estimated voltage magnitude is updated every sample. For a monitoring quality rms value will be calculated once per averaging time on the basis of selected number of half or one-cycle values.

In order to explore the dip duration identification, it is suggested to search automatically the output vectors of rms characteristic in order to indicate values which do not fulfil a given threshold. These values stay in reference to the time axis and indicate dip initiation and voltage recovery. The first activity uncovers influence of the threshold level on dip duration obtained thanks to three applied rms voltage estimation algorithm for given one-cycle window. Second activity aims to compare obtained dip duration for one-cycle window with given threshold 90%. Proposed approach can be treated as an academic off-line calculation in order to uncover the idea of the dip identification using the threshold. Normally, in on-line application, this identification is done automatically, in real time, on the basis of every new sample which does not fulfil requirements for a given threshold. Presented in this section attitude serves as comparison of the threshold level on detected duration time of the dip. Table 8-4 gives a proposition of demonstration algorithm in Matlab dedicated to an influence of a threshold on dip duration. The effects of comparison is presented in Fig. 8.13.

Table 8-4. Demonstration algorithm applying discussed method and comparison of threshold level on dip duration

```
%---------SIGNAL-----------------------------------------------------------------
clear all, close all
load sag_gd;
%sag_gd.mat contain uL1 uL2 uL3 4096 samples
%fs=10240Hz
%it covers 20 cycles (period of fundamental component)
%4096 total number of samples
%2048 samples/ 10cycle
%204.8 samples/ 1cycle, round 204 sample/cycle
x=uL1;
h=plot(t,x)
set(h,'LineWidth',2);
xlabel('time [s]')
ylabel('voltage [V]')
grid on
axis('tight')
%---------INITIAL PARAMETERS-----------------------------------------------------------------
icycle=1/2;      %icycle- executive window width in cycles of fundamental component
fo=50;      %fundamental component 50Hz
To=1/fo;    %one cycle of the fundamental component in [s]
tN=icycle*To;    %executive window width in [s]
N=round(icycle*To/dt)   %executive window width in [samples]
%--------------------------------------------------------------------------

%--------------------------------------------------------------------------
%TIME ANALYSIS - Vrms1- rms voltage: 1-phase, high quality
%--------------------------------------------------------------------------
%Vrms1 - vector of local rms voltage
%calculated on the basis of N samples of the signal
%High quality mode - every next Vrms1 are obtained
%by shifting the window along signal sample by sample.
%Note - first value of Vrms1 can be obtained after recording of
%assumed N samples of executive window (tN in seconds).
%Thus we should rescale time axis in Figure representing rms voltage
%starting from tN and finish with end of the signal ->t1
%For high quality mode we preserve time step in t1 as dt
for k=1:length(x)-N
    k
    n=[k:k+N-1]; %identification of windowed samples
    xN=[x(n)];   %windowed signal samples taken for calculation of local rms
    Vrms1(k)=sqrt(1/N*sum(xN.^2));
end
t1=t(N+1:length(x));
figure
h=plot(t1,Vrms1)
set(h,'LineWidth',2)
xlabel('time [s]')
ylabel('voltage magnitude [V]')
title(['Vrms1: ',num2str(icycle),'-cycle window'])
grid on
axis('tight')
%--------------------------------------------------------------------------

%--------------------------------------------------------------------------
%TIME ANALYSIS - Vrms2 - peak voltage: 1-phase, high quality
%--------------------------------------------------------------------------
%Vrms2 - vector of local rms voltage
%calculated on the basis of N samples of the signal
%High quality mode - every next Vrms2 are obtained
%by shifting the window along signal sample by sample.
%Note - first value of Vrms2 can be obtained after recording of
%assumed N samples of executive window (tN in seconds).
%Thus we should rescale time axis in Figure representing rms voltage
%starting from tN and finish with end of the signal ->t1
%For high quality mode we preserve time step in t1 as dt

for k=1:length(x)-N
    k
    n=[k:k+N-1]; %identification of windowed samples
    xN=[x(n)];   %windowed signal samples taken for calculation of local rms
    Vrms2(k)=1/sqrt(2).*(max(abs(x(n))));
end
t2=t(N+1:length(x));
figure
h=plot(t2,Vrms2)
set(h,'LineWidth',2)
xlabel('time [s]')
ylabel('voltage magnitude [V]')
title(['Vrms2: ',num2str(icycle),'-cycle window'])
grid on
axis('tight')
```

```
%-------------------------------------------------------------------------
%FREQUENCY ANALYSIS - fundamental voltage componnent
%-------------------------------------------------------------------------
switch icycle
case 0.5
p=To/dt;        %p-delta phase shift
m=[0:N*2-1];                %frequency axis in [bin number]
fanalysis=(fs*m)/(N*2);     %frequency axis in [Hz]
m50=50*(N*2)/fs+1;          %bin of 50Hz
for k=1:(length(x)-N);
   k
   n=[k:k+N-1]; %identification of windowed samples
   xN=[x(n),-x(n)]; %special series windowed signal samples taken for FFT
   localspectrumu=fft(xN,N*2);
   %local complex rms voltage of fundamental  component
   fundamental50uc=localspectrumu(m50)*exp(-j*(2*pi/p)*(k-1))./(sqrt(2));
   s1=2/(N); %scale factor for magnitude
   real50u(k)=real(fundamental50uc).*s1;    %real part of local rms voltage of fundamental component
   img50u(k)=imag(fundamental50uc).*s1; %imaginary part of local rms voltage of fundamental component
   s2=180/pi;%scale factor for phase in angle
   phase50u(k)=(angle(fundamental50uc)+pi/2)*s2; %local phase of fundamental component
end
Vrms3=sqrt((real50u).^2+(img50u).^2);
t3=t(N+1:length(x));
otherwise
p=To/dt;        %p-delta phase shift
m=[0:N-1];              %frequency axis in [bin number]
fanalysis=(fs*m)/(N);   %frequency axis in [Hz]
m50=50*(N)/fs+1;            %bin of 50Hz
for k=1:(length(x)-N);
   k
   n=[k:k+N-1]; %identification of windowed samples
   xN=[x(n)];   %windowed signal samples taken for FFT
   localspectrumu=fft(xN,N);
   %local complex rms voltage of fundamental  component
   fundamental50uc=localspectrumu(m50)*exp(-j*(2*pi/p)*(k-1))./(sqrt(2));
   s1=2/(N); %scale factor for magnitude
   real50u(k)=real(fundamental50uc).*s1;    %real part of local rms voltage of fundamental component
   img50u(k)=imag(fundamental50uc).*s1; %imaginary part of local rms voltage of fundamental component
   s2=180/pi;%scale factor for phase in angle
   phase50u(k)=(angle(fundamental50uc)+pi/2)*s2; %local phase of fundamental component
end
Vrms3=sqrt((real50u).^2+(img50u).^2);
t3=t(N+1:length(x));
end
figure
h=plot(t3,Vrms3)
set(h,'LineWidth',2)
xlabel('time [s]')
ylabel('voltage magnitude [V]')
title(['Vrms3: ',num2str(icycle),'-cycle window'])
grid on
axis('tight')
%-------------------------------------------------------------------------

%-------------------------------------------------------------------------
vartreshold=[0.95 0.9 0.85 0.8]; %various treshold level for given icycle
%-------------------------------------------------------------------------
for m=1:4
    treshold=vartreshold(m)
    durationVrms1samples=find(Vrms1<=treshold*Vrms1(1));
    beginVrms1=t1(durationVrms1samples(1))
    endVrms1=t1(durationVrms1samples(length(durationVrms1samples)))
    durationVrms1seconds(m)=endVrms1-beginVrms1
    durationVrms1cycles(m)=durationVrms1seconds(m)/To

    durationVrms2samples=find(Vrms2<=treshold*Vrms2(1));
    beginVrms2=t2(durationVrms2samples(1))
    endVrms2=t2(durationVrms2samples(length(durationVrms2samples)))
    durationVrms2seconds(m)=endVrms2-beginVrms2
    durationVrms2cycles(m)=durationVrms2seconds(m)/To

    durationVrms3samples=find(Vrms3<=treshold*Vrms3(1));
    beginVrms3=t3(durationVrms3samples(1))
    endVrms3=t3(durationVrms3samples(length(durationVrms3samples)))
    durationVrms3seconds(m)=endVrms3-beginVrms3
    durationVrms3cycles(m)=durationVrms3seconds(m)/To
end

h=plot(vartreshold,durationVrms1seconds,'--bs','MarkerEdgeColor','k','MarkerFaceColor','b','MarkerSize',8)
set(h,'LineWidth',2)
hold on
h=plot(vartreshold,durationVrms2seconds,'--gv','MarkerEdgeColor','k','MarkerFaceColor','g','MarkerSize',8)
set(h,'LineWidth',2)
hold on
h=plot(vartreshold,durationVrms3seconds,'--rd','MarkerEdgeColor','k','MarkerFaceColor','r','MarkerSize',8)
set(h,'LineWidth',2)
hold off
xlabel('voltage treshold')
ylabel('dip duration [s]')
title(['Vrms1,Vrms2,Vrms3: ',num2str(icycle),'-cycle window'])
legend('Vrms1','Vrms2','Vrms3')
grid on
axis('tight')
%-------------------------------------------------------------------------
```

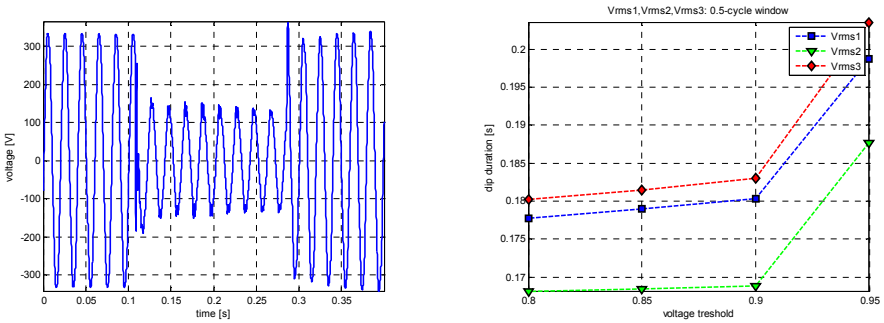

Fig. 8.13. Investigated one-phase signal and comparison of threshold level on dip duration

8.5.Phase-angle jump

In power systems voltage and current is a complex quantity (phasor) which has magnitude and phase. The description of such event as dips is not limited to magnitude variation but includes also phase changes. It has a meaning when we work with sensitive equipment as power converters which use phase-angle information for their firing instant. The phase-angel jump manifests itself as shift in zero-crossing of the instantaneous voltage. In order to define a phase-angle jump, we need to track a difference between a phase-angle before the event (steady state) and a phase-angle during the event. The instantaneous value of the voltage can be calculated using voltage zero-crossing method (time analysis) or from the phase of fundamental component (frequency analysis).

As it was mentioned in the previous section, the voltage "fundamental component" method introduced frequency analysis using FFT application. In a frequency domain, particular components are the complex value represented by magnitude and phase.

In a digital application, we have to consider one additional issue. In a continuous time-domain the instantaneous voltage waveform of fundamental component is considered as a rotating phasor. The rotation is described by rotation operator and consists two components: time operator $exp(-j\omega_0 t)$ and phase operator $exp(-j\psi)$:

$$v_0(t) = V_{max} \cdot sin(\omega_0 t + \psi) \Rightarrow \underline{V(t)} = V \cdot e^{j(\omega_0 t + \psi)} = V \cdot e^{j\omega_0 t} \cdot e^{j\psi} \qquad (8.6)$$

In the point of phase tracking the most important is the phase operator. However, in the digital application using the shifting window, we introduce a rotation operator as complex

mechanism. Thus, in order to identify desirable phase operator we have to “move back” the phasor by correction $exp(-j\omega_0 t)$. In a digital notice, it means exp(-j*(2*pi/p)*(k-1) where $p=T_0/dt$, dt – sampling rate, T_0 – period of fundamental component.

Table 8-5 contains a demonstration algorithm in Matlab realising a phase-angle jump assessment on the basis of fundamental phasor changes. The transition of phase-angle changes is presented in Fig. 8.14. Additionally, the influence of window width on discussed characteristic is shown in Fig. 8.15.

Table 8-5. Demonstration algorithm applying fundamental component method for phase-angle jump calculation

```
%---------SIGNAL----------------------------------------------------------------
clear all, close all
load sag_gd;
%sag_gd.mat contain uL1 uL2 uL3 4096 samples
%fs=I0240Hz
%it covers 20 cycles (period of fundamental component)
%4096 total number of samples
%2048 samples/ 10cycle
%204.8 samples/ 1cycle, round 204 sample/cycle
x=uL1;
h=plot(t,x)
set(h,'LineWidth',2);
xlabel('time [s]')
ylabel('voltage [V]')
grid on
axis('tight')
%---------INITIAL PARAMETERS----------------------------------------------------------------
icycle=1/2;      %icycle- executive window width in cycles of fundamental component
fo=50;      %fundamental component 50Hz
To=1/fo;    %one cycle of the fundamental component in [s]
tN=icycle*To;    %executive window width in [s]
N=round(icycle*To/dt)   %executive window width in [samples]
%-------------------------------------------------------------------------

%-------------------------------------------------------------------------
%FREQUENCY ANALYSIS - Vrmsfundamental voltage componnent
%-------------------------------------------------------------------------
switch icycle
case 0.5
p=To/dt;        %p-delta phase shift
m=[0:N*2-1];                %frequency axis in [bin number]
fanalysis=(fs*m)/(N*2);     %frequency axis in [Hz]
m50=round(50*(N*2)/fs+1);           %bin of 50Hz
for k=1:(length(x)-N);
   k
   n=[k:k+N-1]; %identification of windowed samples
   xN=[x(n),-x(n)]; %special series windowed signal samples taken for FFT
   localspectrumu=fft(xN,N*2);
   %local complex rms voltage of fundamental  component
   s1=2/(N*2); %scale factor for magnitude
   s2=180/pi;%scale factor for phase in angle
   fundamental50uc=localspectrumu(m50)*exp(-j*(2*pi/p)*(k-1))./(sqrt(2)).*s1;
   real50u(k)=real(fundamental50uc);    %real part of local rms voltage of fundamental component
   img50u(k)=imag(fundamental50uc); %imaginary part of local rms voltage of fundamental component
   s2=180/pi;%scale factor for phase in angle
   phase50u(k)=(angle(fundamental50uc)+pi/2)*s2; %local phase of fundamental component as sin
end
Vrms3=sqrt((real50u).^2+(img50u).^2);
t3=t(N+1:length(x));
otherwise
p=To/dt;        %p-delta phase shift
m=[0:N-1];              %frequency axis in [bin number]
fanalysis=(fs*m)/(N);   %frequency axis in [Hz]
m50=round(50*(N)/fs+1);         %bin of 50Hz
for k=1:(length(x)-N);
   k
   n=[k:k+N-1]; %identification of windowed samples
   xN=[x(n)];   %windowed signal samples taken for FFT
   localspectrumu=fft(xN,N);
   %local complex rms voltage of fundamental  component
   s1=2/(N); %scale factor for magnitude
   s2=180/pi;%scale factor for phase in angle
   fundamental50uc=localspectrumu(m50)*exp(-j*(2*pi/p)*(k-1))./(sqrt(2)).*s1;
   real50u(k)=real(fundamental50uc);    %real part of local rms voltage of fundamental component
   img50u(k)=imag(fundamental50uc); %imaginary part of local rms voltage of fundamental component
   phase50u(k)=(angle(fundamental50uc)+pi/2)*s2; %local phase of fundamental component as sin
end
Vrms3=sqrt((real50u).^2+(img50u).^2);
t3=t(N+1:length(x));
end
%-------------------------------------------------------------------------
figure
h=plot(t3,Vrms3)
set(h,'LineWidth',2)
xlabel('time [s]')
ylabel('voltage magnitude [V]')
title(['Vrms3: ',num2str(icycle),'-cycle window'])
grid on
axis('tight')
figure
h=plot(t3,phase50u)
set(h,'LineWidth',2)
xlabel('time [s]')
ylabel('phase [deg]')
title(['phase: ',num2str(icycle),'-cycle window'])
grid on
axis('tight')
phase50uanglejump=phase50u-phase50u(1);
figure
h=plot(t3,phase50uanglejump)
set(h,'LineWidth',2)
xlabel('time [s]')
ylabel('phase-angle jump [deg]')
title(['phase-angle jump: ',num2str(icycle),'-cycle window'])
grid on
axis('tight')
```

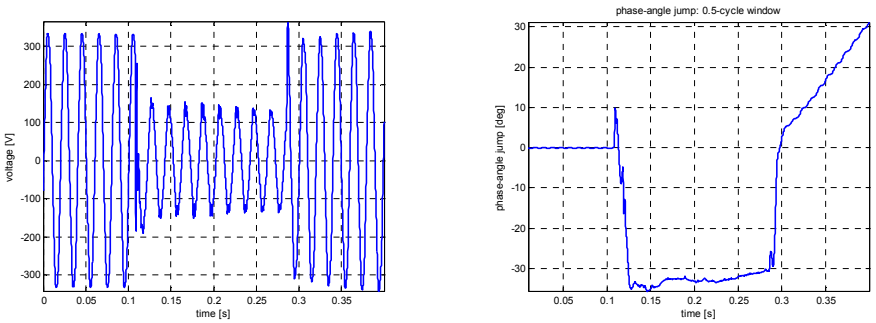

Fig. 8.14. Investigated one-phase signal and its phase-angle jump

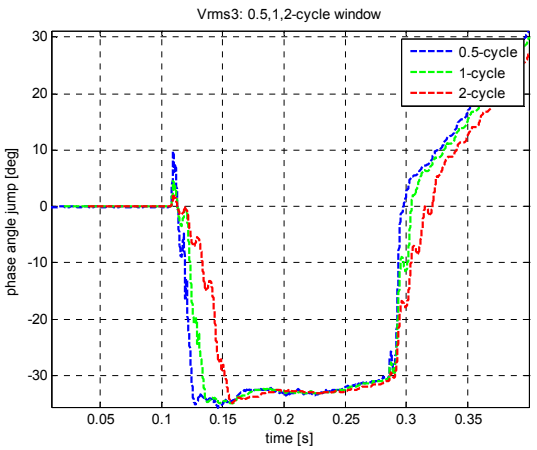

Fig. 8.15. Influence of the window width on on transition of phase-angel jump characteristic

8.6.Monitoring mode in voltage dips assessment

The previous sections described three algorithms dedicated to voltage magnitude deterioration: rms voltages and peak voltages, associated with a direct time analysis, and fundamental voltage component using frequency analysis. No mater what kind of method was selected to apply, the mechanism of tracking voltage along the signal ,which leads to time characteristic of magnitude or phase variation in time, was the same – shifting an executive window. It means that the main algorithm responsible for magnitude estimation was applied only for a particular portion of samples, designated by the window, many times for its particular location. Finally, we have achieved many half or one-cycle local values of rms voltage associated with a position of the window along time axis. Representation of

these local rms values along the time axis gives desirable characteristic of voltage variation during the event.

Until now, we have applied high quality calculation, where the shift of the window was fine i.e. sample by sample. In a practical adaptation of the rms estimation high quality mode is too time-consuming and requires computational power. Thus, for monitoring mode, we often reintroduce the ideas of rms algorithms as the rms value is calculated once per cycle and can be grouped and averaged in interval of 200ms or 10 minutes [3],[4],[6]. In a monitoring mode the shift is "fat" i.e. window by window with an optional averaging period or not . Please notice that this time, the first value of estimated rms voltage is localized in time moment equals *N*dt* where *dt* is the sampling rate. The next points of desirable rms voltage characteristic are calculated on the basis of fragments of the recorded data, designated by shifting cycle-by-cycle window. Thus, we need to recalculate the time axis using "fat" time step *N*dt*, *t*=[*N*dt, 2*N*dt, …,k*N*dt…*]. The description of the idea is depicted in Fig. 8.16. In comparison with Fig. 8.3, we can observe rough estimation, that however saves the computational power for calculation.

Additionally, the averaging time is introduced concerning one value for selected numbers of cycles (half-cycles) i.e. 200ms averaging time means that we achieve one value of rms from 10 one-cycle values or 20 half-cycles values [3],[4],[6].

In order to close the idea, Table 8-6 and Fig. 8.17 show demonstration algorithm or classical rms calculation working in a monitoring mode without additional averaging. To understand the difference between high-quality and monitoring mode, we recommend comparing Fig. 8.17 and Fig. 8.5.

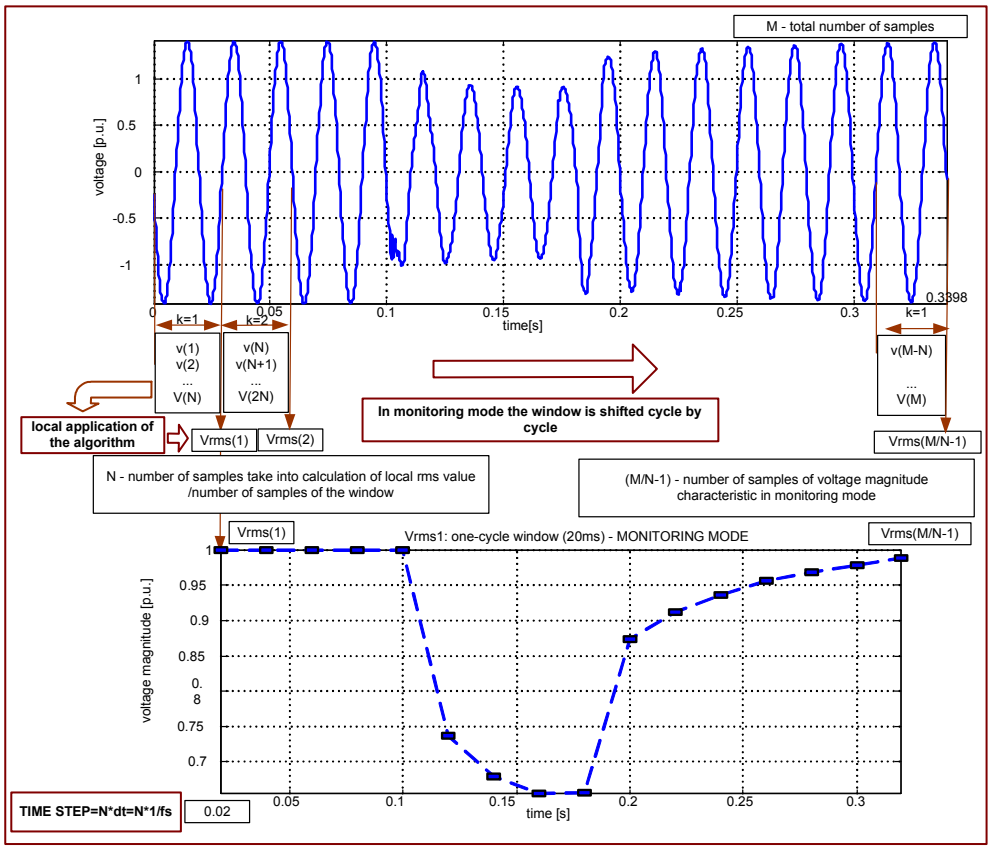

Fig. 8.16. Mechanism of rms voltage characteristic in monitoring mode without averaging

Table 8-6. Demonstration algorithm applying classical rms calculation method in monitoring mode without additional averaging

```
%---------SIGNAL----------------------------------------------------------------
clear all, close all
load sag_gd;
%sag_gd.mat contain uL1 uL2 uL3 4096 samples
%fs=10240Hz
%it covers 20 cycles (period of fundamental component)
%4096 total number of samples
%2048 samples/ 10cycle
%204.8 samples/ 1cycle, round 204 sample/cycle
x=uL1;
h=plot(t,x)
set(h,'LineWidth',2);
xlabel('time [s]')
ylabel('voltage [V]')
grid on
axis('tight')
%---------INITIAL PARAMETERS----------------------------------------------------------------
icycle=1;      %icycle- executive window width in cycles of fundamental component
fo=50;      %fundamental component 50Hz
To=1/fo;    %one cycle of the fundamental component in [s]
tN=icycle*To;    %executive window width in [s]
N=round(icycle*To/dt)   %executive window width in [samples]
%-------------------------------------------------------------------------

%-------------------------------------------------------------------------
%TIME ANALYSIS - Vrms1- rms voltage: 1-phase, monitor mode
%-------------------------------------------------------------------------
%Vrms1 - vector of local rms voltage
%calculated on the basis of N samples of the signal
%High quality mode - every next Vrms1 are obtained
%by shifting the window along signal sample by sample.
%Note - first value of Vrms1 can be obtained after recording of
%assumed N samples of executive window (tN in seconds).
%Thus we should rescale time axis in Figure representing rms voltage
%starting from tN and finish with end of the signal ->t1
%For high quality mode we preserve time step in t1 as dt
%For monitoring mode time step equals number of cycles -> window by widnow
l=1;    %monitoring mode storage initial
for k=1:N:length(x)-N
    k
    n=[k:k+N-1]; %identification of windowed samples
    xN=[x(n)];   %windowed signal samples taken for calculation of local rms
    Vrms1(l)=sqrt(1/N*sum(x(n).^2));
    l=l+1;
end
t1=t(N+1:N:length(x));
figure
h=plot(t1,Vrms1,'--bs','MarkerEdgeColor','k','MarkerFaceColor','b','MarkerSize',8)
set(h,'LineWidth',2)
xlabel('time [s]')
ylabel('voltage magnitude [p.u.]')
title(['Vrms1: ',num2str(icycle),'-cycle window'])
grid on
axis('tight')
%-------------------------------------------------------------------------
```

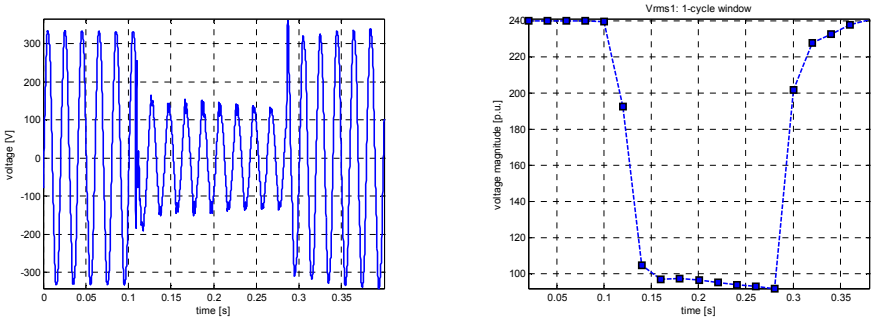

Fig. 8.17. Investigated one-phase signal and its rms trend using one-cycle classical rms algorithm in monitoring mode without additional averaging

8.7.Dip transfer in power systems

The prominent number of dips in power systems comes from short-circuit faults which can appear in a different level of the system structure: transmission system faults, remote distribution systems faults, local distribution system faults. Other origins of the dips may have their sources in a starting process of large motors, short interruption and fuses [1],[2],[3],[4].

According to the standards, dips can be entirely defined by the magnitude and duration. Considering the duration of dips, we can distinguish self-decaying events and events determined by fault-clearing equipments. Generally speaking, the faults in transmission systems are cleared faster than faults in distribution systems. In transmission systems, the critical fault-clearing time is rather small. Thus, fast protection and fast circuit breaker are essential. Also transmission and subtransmission systems are normally operated as a grid, requiring a distance protection or a differential protection, both of which are rather fast. The principal form of a protection in distribution systems are overcurrent protection. This often requires some time-grading which increases the fault –clearing time. An exception constitutes systems in which current-limiting fuses are used that have the ability to clear a fault within one half-cycle [1],[2],[3],[4].

The drop of rms voltage during the dips depends on a few conditions. One of the crucial issue is relation between the location of the fault and the location of observation in the system structure i.e. point of common coupling (PCC). A general rule indicates significant influence of the dips on the customers grouped at the same level of voltage as appearing fault. Further distribution of the dip depends on the location of the fault in the system structure and the presence of the impedance of the transformer. Thus, a short-circuit fault in local distribution networks (medium or low voltage) typically leads to deep dips whpse injury every customer grouped in near regions. This is due to small impedance taken into consideration which comes only from impedance of distribution feeders often with limited length. These dips will not cause much voltage drop for the customers fed at the sub-transmission and transmission level. The impedance of the transformers between the distribution and subtransmission, and further, between the sub-transmission and transmission level are large enough to considerably limit the voltage drop at the high voltage side of the transformer. However, the fault in the sub-transmission system will cause a deep dip in the subtransmission substation and for all customers fed from this substation. The

dips will be visible at every lower voltage side of the substation. Customers working on the transmission voltage level will experience a shallow dip, again due to the transformer impedance. Finally, the fault in the transmission system will cause a serious dip for fed substations bordering the faulted line. This dip is then transferred down to all customer fed from these substations [1],[2],[3],[4].

In order to emphasize mentioned general rules of the dips transfer in the power systems, we have attached an example of the power network with possible fault position Fig. 8.18 and the table of scenarios dedicated to dips influence Table 4-1. It must be mentioned that given characterization has a general nature and does not include some specific situations as distributed generation.

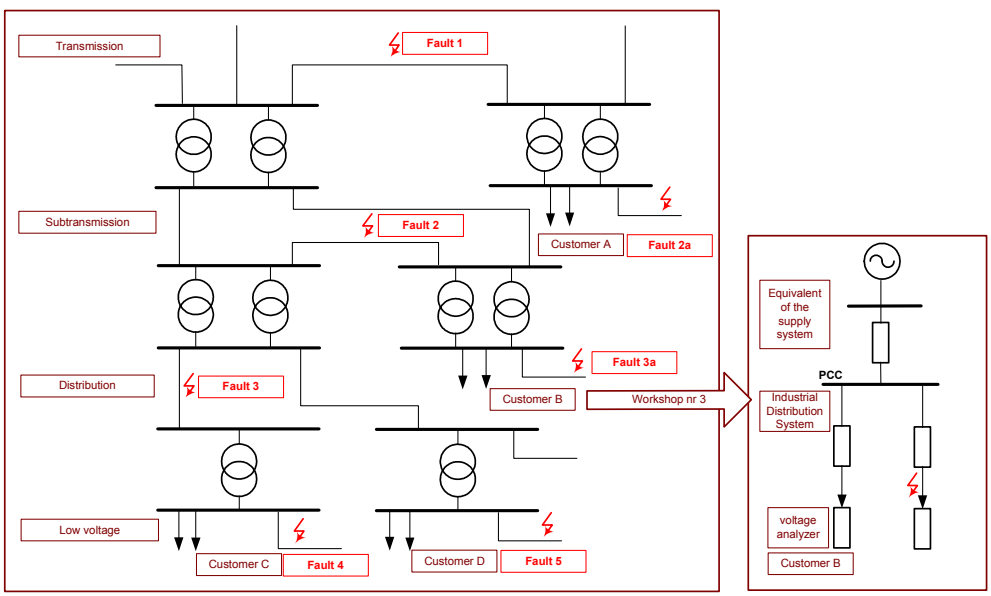

Fig. 8.18. Example of power network with possible fault position scenarios dedicated to general dips transfer

Table 8-7 Possible scenarios of dips transfer in power systems from Fig. 8.18 referring to fault position

	Label Fig. 8.18	Customer A	Customer B	Customer C	Customer D
Transmission	Fault 1	deep dip	deep dip	deep dip	deep dip
Subtransmission	Fault 2	not much	deep dip	deep dip	deep dip
Subransmission/ industrial network	Fault 2a	deep dip	not much	not much	not much
Distribution	Fault 3	not much	not much	deep dip	deep dip
Distribution/ industrial network	Fault 3a	not much	deep dip	not much	not much
Distribution utility network	Fault 4	rather not notice	rather not notice	deep dip	shallow dip
Distribution utility network	Fault 5	rather not notice	rather not notice	shallow dip	deep dip

As an example, we would like to consider an often met scenario – a fault in a local distribution network. Range of the investigation is scoped around influence on "neighbour" customer. It corresponds to scenario **Fualt 3a** from Fig. 8.18 and Table 4-1, where measurements are localized at customer, fed by a feeder without the fault. Considering the mentioned scenario, we can scope on some details as influence of the local parameters on character of the dips observed by the customer, especially relation between the dips and length of the faulted feeder as well as relation between the dips and kind of fault. The aim of the activities is to familiarize with a selected origin of the dips. In order to perform the investigations we have prepared the model of the simplified diagram of the network illustrated in Fig. 8.19. Presented here diagram was modelled in Matlab (R13 6.5) Simulink environment using SimPowerSystem Blockset [7] ,[8]. The model is available at http://eportal.eny.pwr.wroc.pl/ .

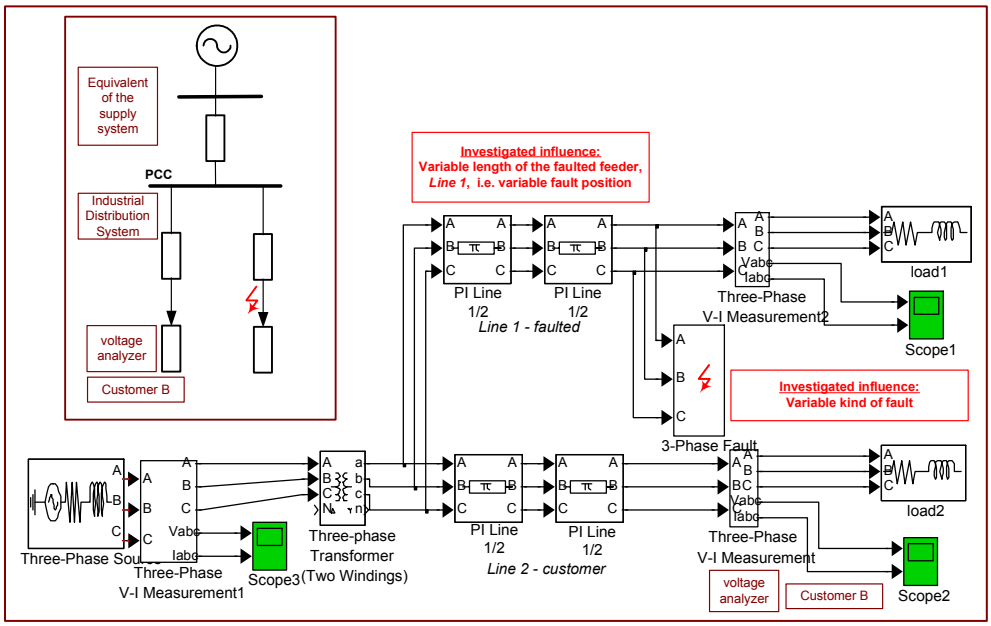

Fig. 8.19. Simplified diagram of the investigated network and its model in Simulink SimPowerSystem Blockset

The system is described by an initial short-circuit apparent power 3GVA and a voltage level of 110 kV. The transformer is a two-winding (delta-wye-isolated) 110/15-kV distribution transformer with a nominal power 10MVA. L1 and L2 are typical overhead lines. Both lines supply the RL loads. The line 2 has a 5km length and fed observed industrial customer. In a point of numerical reasons, the lines are modeled as two Pi-line components. The short circuit occurs at the end of the line L1.

The investigation is aimed at:

- the influence of the length of ***Line 1 (faulted line)*** on the dips injured Customer B: suggested range L1=1km, L1=5km,

- the influence of the ***kind of fault*** on the dips injured Customer B: suggested range – A-GND one-phase fault with ground, A-B two-phase fault.

The investigated signals comes from the observation made by Customer B. In model it is realized by *Scope 2*. Setup of the Scope considers sample time 2e-4s (0.2ms). For a digital calculation, it is very important information which allows defining sampling frequency *fs=1/(0.2ms)=5kHz*. The time axis is automatically saved in workspace. Selected range of the observation *is (0-0.6s)*.

As an example Fig. 8.20 represents the character of the dip for the same kind of a fault, A-GND, but for different fault location L1=1km vs L1=5kme. Estimation method utilizes classical rms definition in high-quality mode.

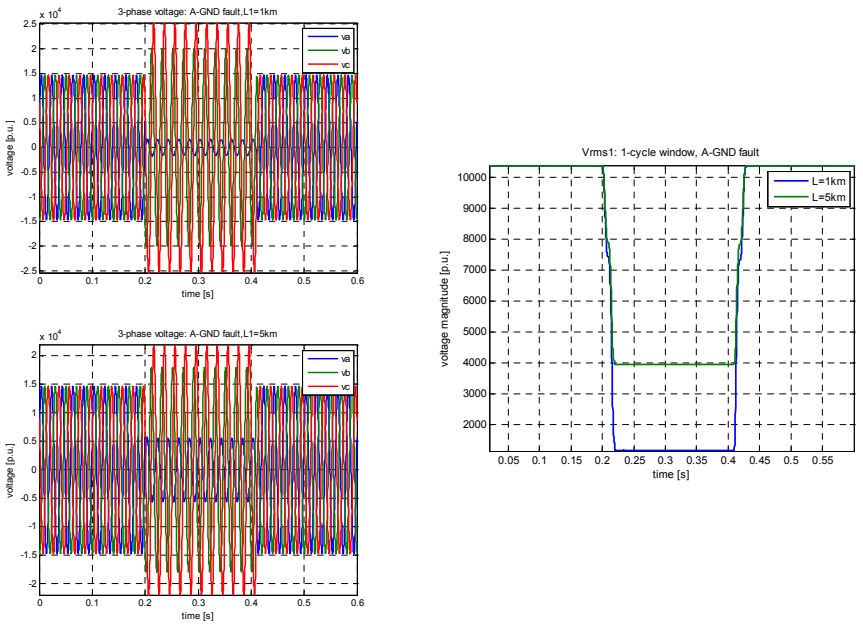

Fig. 8.20. Influence of distance of faulted line on observed dip in grid point in neighbour line

Fig. 8.21 depicts the influence of the kind of fault in faulted line on observed dip in grid point in neighbour line for the same length of faulted line which equals 1km. Estimation method utilizes classical rms definition in high quality mode.

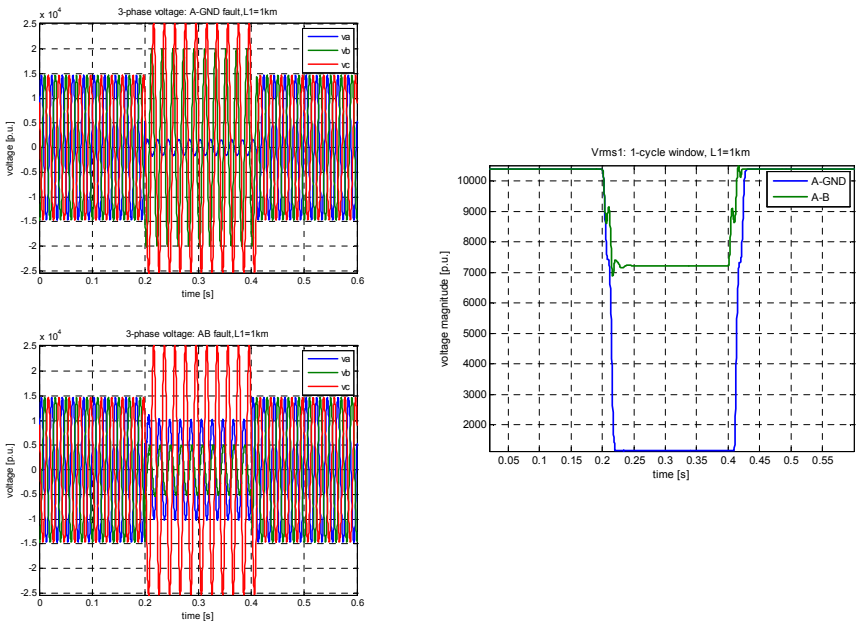

Fig. 8.21. Influence of kind of fault in faulted line on observed dip in grid point in neighbour line

8.8.Literature

[1] Bollen M.H.J., *Understanding Power Quality Problems. Voltage sags and interruptions*, IEE Press Series on Power Engineering, 2000.

[2] Dugan R. C. et al, *Electrical Power Systems Quality*, McGraw-Hill, 2004.

[3] Sankaran C., *Power Quality*, CRC Press, 2002.

[4] *Power Quality Application Guide. Chapter 5. Voltage Disturbances*. The European Copper Institute, Leonardo da Vinci European Program on Power Quality Assessment.

[5] Łobos T., Sikorski T., Amaris H., Alonso M., Florez D., *Classical and alternative methods to voltage quality monitoring*, Computer Application in Electrical Engineering, Poznan, 2009.

[6] IEC 61000-4-30:2008, *Electromagnetic compatibility (EMC): Testing and measurement techniques -Power quality measurement method*.

[7] *SimPowerSystems User's Guide*. The Math Works Inc., 2006.

[8] P. Janik, *Charakterystyka zakłóceń jakości energii elektrycznej za pomocą zaawansowanych metod analizy sygnałów*, in Polish, Ph.D. Thesis, 2005.

9. Computational application of power quality assessment: harmonics

The previous chapter was dedicated to dips assessment, as the representative of events. It is worth emphasising that main division of power quality disturbances includes events as well as variations. Events are sudden disturbances with a beginning and an ending. To measure the events, triggering process must be involved, usually using a threshold. Variations are steady-state or quasi-steady-state disturbances that require continuous measurements.

With reference to more classical power engineering, the measurement of variations is similar to metering of the energy consumption (i.e., continuous), whereas the measurement of events is similar to the functioning of a protection relay (i.e., triggered). Neglecting the purpose of the measurements, every process of quantification starts from devices responsible for voltage and current measurements. The difference is in the further processing and application of the measured signals. The results of power quality monitoring are not used for any automatic intervention in the system. Exceptions are the measurements as part of power quality mitigation equipment, but such equipment is more appropriately classified as protection or control equipment. Fig. 9.1 depicts a general scheme of power quality measurements with distinction between variation and event .

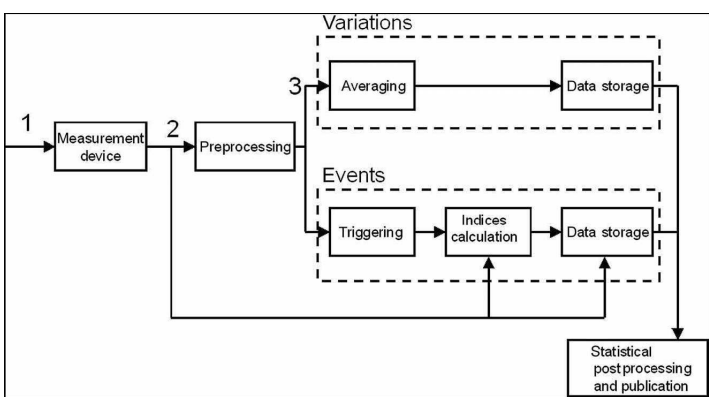

Fig. 9.1. General scheme of power quality measurements: (1) voltage or current in system; (2) sampled and digitized voltage or current; (3) quantity for further processing [2]

This chapter is dedicated to variations. The process of variations assessment requires calculation of appropriate characteristics. This may be the rms voltage trend, the frequency trend or the

spectrum. Due to a continuous character of measurement some averaging conditions over a certain interval must be introduced. The calculation of rms-voltage, the frequency or the spectrum in high-quality mode would generate huge number of data with high requirements for data storage and computational power. Thus, for variations much more practical approach consider monitoring-mode with additional parameter called averaging time. For example, if averaging time equals 200ms i.e. 10 periods of fundamental 50Hz component, we achieve one averaged value of rms from ten one-cycles values, or one estimated frequency value from 10-cycle, or at least one spectrum obtained on the basis of 10-cycle [1],[2].

The standard document IEC 61000-4-30 [4] prescribes the following intervals: 10 or 12 cycles, 150 or 180 cycles, 10 min, and 2 h. Some monitors use different window lengths. Some monitors also give maximum and minimum values obtained during each interval. Some monitors do not take the average of the characteristic over the whole interval but a sample of the characteristic at regular intervals, for example, the spectrum obtained from one cycle of the waveform once every 5 min. Further postprocessing consists of the calculation of representative statistical values (e.g., the average or the 95 percentile) over longer periods (e.g., one week) and over all monitor locations. The resulting values are referred to as site indices and system indices, respectively [2].

9.1.Harmonics distortion and Fourier series parameterization

Waveform distortion includes all deviations of the voltage or current waveform from the ideal sine wave. But variations in magnitude and frequency are not considered as waveform distortion although a complete distinction between the different types of variations is not possible. A number of different forms of waveform distortion can be distinguished:

- harmonic,
- interharmonic,
- nonperiodic distortion.

In most studies, only the harmonic distortion is considered. Nonharmonic distortion (interharmonics and nonperiodic distortion) is much harder to quantify through suitable parameters and it is regularly neglected. Another reason for neglecting nonharmonic distortion is that harmonic distortion dominates in most cases. Coming back to the harmonics we can distinguish odd-harmonics and even-harmonics. The odd-harmonics manifests itself symmetrically for the positive and negative half of sine wave. Odd-harmonic distortion is typically dominant in supply voltage and load current. The result of even-harmonic distortion is that positive and

negative half-cycles of the signal are no longer symmetrical. Even-harmonic distortion of voltage or current is normally rather small.

The measurement of harmonic distortion is defined in two IEC standards: IEC 61000-4-7 [5] and IEC-61000-4-30 [4]. The first one defines the way in which harmonic current distortion shall be measured when comparing equipment emission with the emission limit. The latter document defines the way in which voltage quality shall be measured.

According to the IEC standards, the Fourier series shall be obtained over a rectangular window with a length equal to 10 cycles in a 50-Hz system and equal to 12 cycles in a 60-Hz system. However we have to realize that the measurement systems may use different sampling rate. Thus, given 10-cycle interval would contain different number of samples, more for high sampling rate, and less for low sampling rate. Here it is worth noticing that in pair with condition given by IEC runs IEEE document IEEE Standard Common Format for Transient Data Exchange (COMTRADE) for Power Systems [6]. This document gives some hints for sampling rate and number of samples in one-cycle of basic components, that can be easily recalculate for 10 cycles, Fig. 9.2.

Samples/cycle	*f* for 60 Hz	*f* for 50 Hz
384	23040	19200
192	11520	9600
128	7680	6400
96	5760	4800
64	3840	3200
48	2880	2400
32	1920	1600
24	1440	1200
16	960	800
12	720	600
8	480	400
6	360	300
4	240	200

Samples/cycle	*f* for 60 Hz	*f* for 50 Hz
3200	192000	160000
1600	96000	80000
800	48000	40000
640	38400	32000
400	24000	20000
320	19200	16000
200	12000	10000
160	9600	8000
128	7680	6400
100	6000	5000
80	4800	4000
64	3840	3200
50	3000	2500
40	2400	2000
32	1920	1600
20	1200	1000
16	960	800
10	600	500
8	480	400
4	240	200

Fig. 9.2. Sampling rates for 50Hz system and 60Hz system with its relations to number of samples in one-cycle of fundamental component [6]

The assessment of the harmonic and interharmonic distortion is based on the discrete Fourier spectrum. The output of the discrete Fourier transform consists of a number of frequency

components, both harmonics and interharmonics. The efficient assessment of the spectrum requires some initial calculation and preparation in order to associate the output of Fourier series with signal parameters. Main activities are scoped around frequency bin specification. An undermentioned example shows a required initial calculation so that performed Fourier series might have a physical meaning.

Example: initial calculation for Fourier series parameterization

Given: sampling rate f_S=*4kHz*, system f_0=*50Hz*, interval *10-cycle*

Searched: a number of samples in the interval and a total number of frequency bins ***N***=*?*,frequency resolution of DFT algorithm ***dfF***=*?*, frequency axis ***f***=*[….]*, maximum order of harmonics ***H***=*?*, frequencies of particular harmonics ***hf,*** index of the harmonics at the frequency axis ***nfch***=*[…].*

Answer:

Referring to Fig. 9.2 for given sampling rate f_S=*4kHz* we have 80 samples per fundamental component 50Hz.

The interval includes 10 cycles, thus for a calculation of DFT we take ***N***=*10x80=800* samples.

Frequency resolution is then ***dfF***=f_S*/N=4000/800=5Hz*.

According to "Nyquist theory" frequency observation range is limited to **1/2 f_S**=2kHz. Thus, we can generate the frequency bins for the frequency axis ***f***=*[0:dfF: 1/2 f_S]=[0:5:2000] – length of frequency axis is 401 bins.*

Please notice that total number of frequency bins is N=800 and the length of frequency observation is limited to 401 bins. Remember that performing the DFT, you achieve the information about positive and negative part of frequency axis. **For the real signal the spectrum is symmetrical and desirable information of the spectrum can be reached from the positive part of frequency axis – in case of DFT algorithm it is first N/2+1 elements.**

Maximum order of harmonics can be calculated as ***H***=*(1/2fs)/f_0=2000/50=40.*

Frequencies of particular harmonics ***hf***=[1:1:H]*f0=[50,100,150….2000] in Hz.

Index of the harmonics in the linear spectrum ***nfch***=*([1:1:H]*f_0/dfF)+1*=[11,21, …. 401]

Finally, frequency bin is characterised which depicts Fig. 9.3.

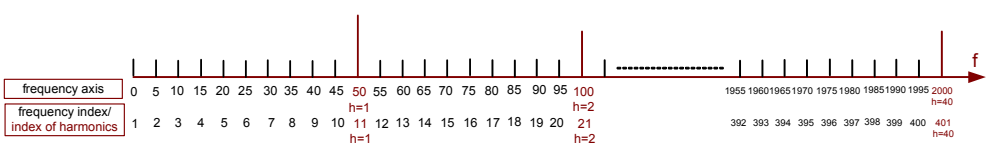

Fig. 9.3. Example of frequency bins characterisation

Some additional comments:

The result of applying the DFT is a spectrum with 5-Hz spacing between frequency components. The spectrum thus contains both harmonics and interharmonics.

We can distinguish the spectrum estimation for voltage and current. The oltage quality is how the network affects the customer or the load; the current quality is how the customer or load affects the network. A similar distinction holds for waveform distortion: the distorted voltages affect the customer equipment; distorted currents affect the network components.

9.2.Investigated phenomena

Main activities in this chapter are concentrated on the investigation of waveform distortion caused by very specific non-linear load which is dc-arc funace. An electric arc furnace (EAF) is a furnace that heats charged material by means of an electric arc. Arc furnaces range in size from small units of approximately one ton capacity (used in foundries for producing cast iron products) up to about 400 ton units used for secondary steelmaking. Arc furnaces used in research laboratories and by dentists may have a capacity of only a few dozen grams. Electric arc furnace temperatures can be up to 1,800 degrees Celsius. Arc furnaces differ from induction furnaces in that the charge material is directly exposed to the electric arc, and the current in the furnace terminals passes through the charged material. A typical dc arc furnace plant and an example of practical realization is shown in Fig. 9.4.

From the electrical point of view, a furnace plant consists of dc arc furnace connected to a medium volt-age ac busbar with two parallel thyristor rectifiers that are fed by transformer secondary winding with Δ and Y connection, respectively. The medium voltage busbar is connected to the high voltage busbar with a HV/MV transformer whose wind-ings are Y-Δ connected. The power of the furnace is 80 MW. The other parameters are: transformer T_1-80 MVA, 220kV/21kV; transformer T_2- 87 MVA, 21kV/0.638kV/0.638kV. Some filters are provided in the plants.

In the dc arc furnace, the presence of the ac/dc static converter and the random motion of the electric arc, whose non linear and time-varying nature is known, are responsible for dangerous perturbations, in particular waveform distortions and voltage fluctuations. In particular, the behaviour of the DC arc furnace can lead to the aperiodicity of AC electrical quantities, namely voltage and current at MV busbar. The phenomena correlated to the arc behavior are very complex. In [7],[8] it has been shown that the DC arc voltage waveform has the aperiodic and

irregular behaviour that characterizes every chaotic phenomenon. As an example, Fig. 9.5 shows an example of current waveform and voltage waveform at MV busbar.

a) b)

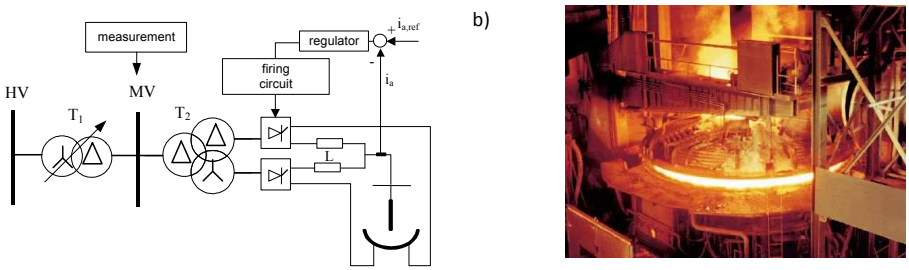

Fig. 9.4. Dc-arc furnace plant (a) and an example of practical realization of arc furnace (b)

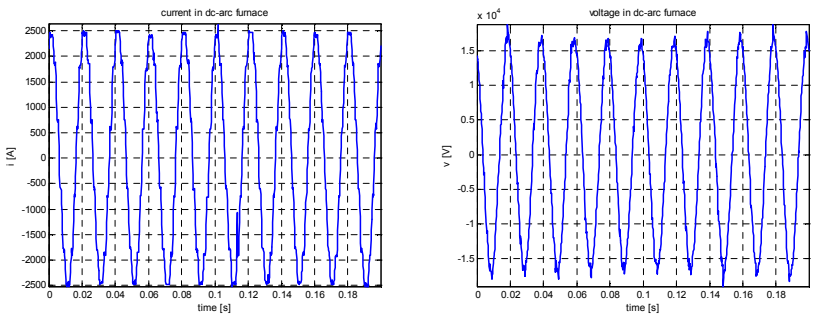

Fig. 9.5. Fragments of current and voltages at MV busbar of dc-arc furnace plant [7],[8]

10-cycle interval of one-phase current (*i*) and voltage (*u*) at MV busbar, with sampling rate equals 5kHz is stored in ***DCArcFurnacemeasure0_02.mat***. This file contains also some additional utilizing parameters as: time vector (*t*), sampling rate f_S=5kHz, and time step (time resolution) ($dt=1/f_S$). The file is available at http://eportal.eny.pwr.wroc.pl/

9.3.“Linear” spectrum estimation using FFT:

Spectrum estimation is considered as a digital representative of continuous “linear” spectrum, which includes whole spectrum components, including harmonics and interharmonics. Table 9-1 consists of demonstration algorithm applying FFT in Matlab in order to calculate the spectrum of the voltage in example of investigated dc-arc furnace plant.

Table 9-1. Demonstration algorithm applying FFT in order to reveal “linear” spectrum

```
%---------SIGNAL-----------------------------------------------------------------
clear all, close all
cd ..
cd Data
load DCArcFurnacemeasure0_02.mat;
cd ..
cd Programs
%file contains 10-cycles 50Hz of dc-arc furnace measured signals:
%sampling rate fs=5kHz;
%Thus we have 100 samples per cycle
%         and 1000 total number of samples in 10 cycles
%i - current,
%u - voltage,
%Additionally:
%fs=5000; [Hz] - sampling rate
%dt=1/fs; [s] - sampling interval
%t-time vector [0:dt:0.2-dt];

x=u;
disp('-----------------------ANALYSED SIGNAL-------------------------------------------------------------')
disp(' ')
disp('CONFIRMATION OF SAMPLED DATA:')
disp(['Sampling frequency fs=',num2str(fs),' Hz'])
disp(['Time step dt=',num2str(dt),' s'])
disp(['End of signal in samples:',num2str(length(x)),' '])
disp(['End of signal in seconds:',num2str(length(x)*dt),' s'])
figure
h=plot(t,x);
set(h,'LineWidth',2);
xlabel('time [s]')
ylabel('u [V]')
title('voltage in dc-arc furnace')
grid on
axis('tight')

%--------------------------------------------------------------------------

%---------INITIAL PARAMETERS-----------------------------------------------------------------
f0=50; %[Hz];    %fundamental component
N=length(x); %number of frequency bins
dfF=fs/(N);  %frequency resolution
%--------------------------------------------------------------------------

%--------------------------------------------------------------------------
%FREQUENCY ANALYSIS
%--------------------------------------------------------------------------
X=fft(x,N);  %Fourier spectrum (positive and negative frequencies)
X_amp=abs(X)*(2/N);          %magnitude spcectrum with scaling factor
X_amp_positive=X_amp(1:1:N/2+1); %magnitude spcectrum only for positive f
f_positive=dfF*(0:1:N/2);          %positive f
%full range of frequency observation 0-fs/2Hz
fc1=0;
fc2=fs/2;
nfc1=round(fc1/dfF)+1;
nfc2=round(fc2/dfF)+1;
figure
h=plot(f_positive(nfc1:nfc2),X_amp_positive(nfc1:nfc2));
set(h,'LineWidth',2);
xlabel('f[Hz]')
ylabel('magnitude');
%title('spectrum of current in dc-arc furnace')
title('spectrum of voltage in dc-arc furnace')
grid on;
%zoom in frequency 0-800Hz
fc1=0;
fc2=800;
nfc1=round(fc1/dfF)+1;
nfc2=round(fc2/dfF)+1;
%zoom in magnitud 0-400
Ampc1=0;
Ampc2=400;
figure
h=plot(f_positive(nfc1:nfc2),X_amp_positive(nfc1:nfc2));
set(h,'LineWidth',2);
xlabel('f[Hz]')
ylabel('magnitude');
%title('spectrum of current in dc-arc furnace - zoom')
title('spectrum of voltage in dc-arc furnace - zoom')
axis([fc1, fc2, Ampc1, Ampc2])
grid on;
%--------------------------------------------------------------------------
```

After calculation of FFT we obtain a set of the frequency component concentrated on every 5Hz frequency bin including its magnitude and phase. Fig. 9.6 and Fig. 9.7 shows magnitude spectrum of voltage and current, respectively. The next activities in assessment of the frequency component is separation of harmonics and interharmonics.

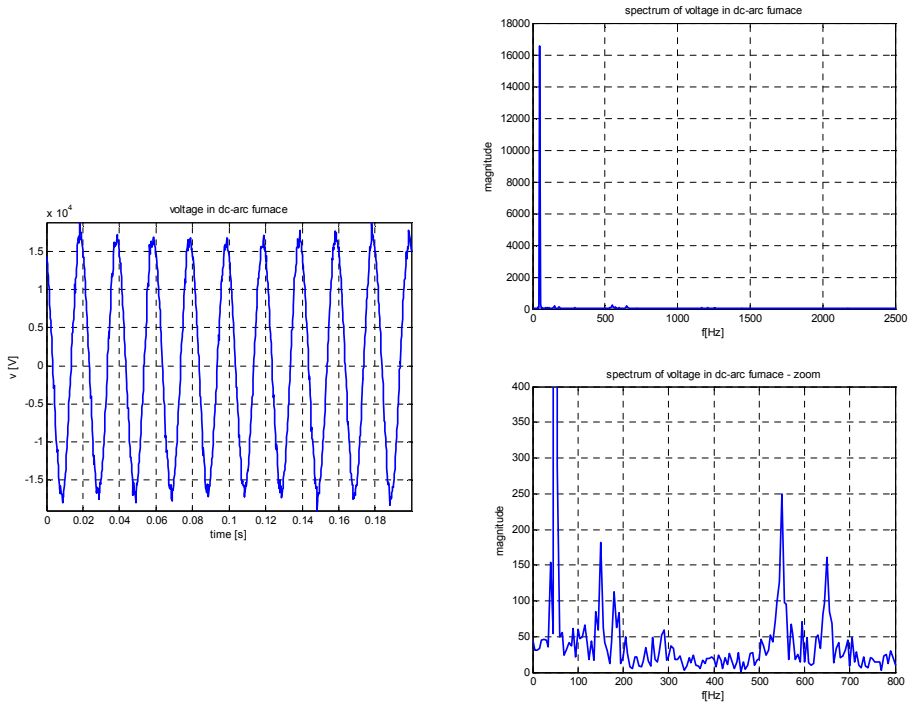

zoom:(0-400)V – (0-800)Hz

Fig. 9.6. Investigated one-phase voltage signal in dc-arc furnace plant and its “linear” spectrum using FFT

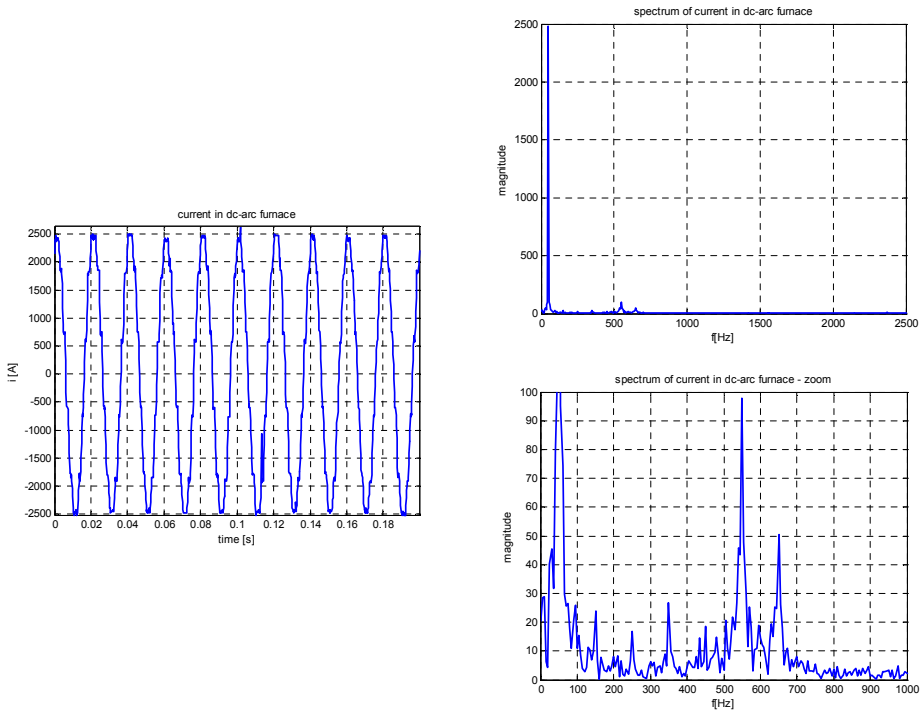

zoom:(0-100)A – (0-800)Hz

Fig. 9.7. Investigated one-phase current signal in dc-arc furnace plant and its “linear” spectrum using FFT

9.4.Harmonics and subdivision into even and odd harmonics

The output of the discrete Fourier transform consists of a number of frequency components, both harmonics and interharmonics. However, the harmonics are only the integral multiplication of fundamental component: 1-st harmonic is 1*50Hz, 2-nd harmonic is 2*50Hz, 3-rd harmonic is 3*50Hz etc. Additionally, the harmonics can be subdivided into even and odd harmonics. Even-harmonic distortion of voltage or current is normally rather small. In many cases odd-harmonics have significant meaning.

Literature provides an additional index in order to depict and summarize a harmonics distortion effect [1],[2],[3],[4],[5]. It is called total harmonic distortion index ***THD*** define as:

$$THD = \frac{\sqrt{\sum_{h=2}^{H} C_h{}^2}}{C_1} * 100\% \tag{9.1}$$

where C_h – magnitude of *h* harmonic (can be voltage or current), C_1 – magnitude of fundamental (*first* harmonic)

The harmonic spectrum can be further subdivided into even harmonics and odd harmonics with their corresponding THD definitions. The total even-harmonic distortion ***THDeven*** may be defined as:

$$THDeven = \frac{\sqrt{\sum_{h=2}^{H} C_{2*h}^2}}{C_1} * 100\% \tag{9.2}$$

where C_{2h} – magnitude of even harmonic, C_1 – magnitude of fundamental (*first* harmonic)

The total odd-harmonic distortion ***THDodd*** may be defined as:

$$THodd = \frac{\sqrt{\sum_{h=2}^{H} C_{2*h-1}^2}}{C_1} * 100\% \tag{9.3}$$

where C_{2h-1} – magnitude of odd harmonic, C_1 – magnitude of fundamental (*first* harmonic)

The confirmation of the proper calculation can use below relations:

$$THD^2 = THDodd^2 + THDeven^2 \;\; ; \;\; THD \approx THDodd \tag{9.4}$$

Activities: Perform initial calculation for Fourier series parameterization

Given: sampling rate f_S=*5kHz*, system f_0=*50Hz*, interval *10-cycle*

Aim: According to the previous example of the initial calculation for a number of samples in the interval and total number of frequency bins ***N***=*?*,frequency resolution of DFT algorithm ***dfF***=*?*, the frequency axis ***f***=*[….]*, maximum order of harmonics ***H***=*?*, frequencies of particular harmonics ***hf,*** index of the harmonics at the frequency axis ***nfch***=*[…]*.

Answer: An expected answer is included in the figure below, Fig. 9.8

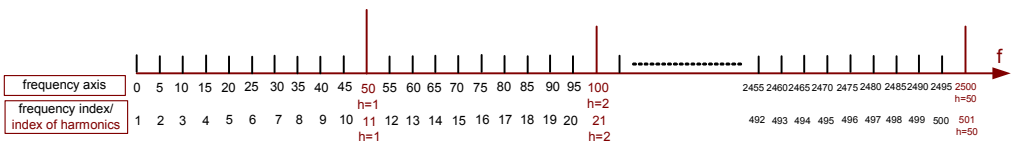

Fig. 9.8. Frequency bins characterization for calculation of investigated voltage and current in example of dc-arc

A definition of frequency bin in “linear” spectrum allows to reveal harmonics, even harmonics and odd harmonics. In the presented example, harmonics [50,100,150,…2500]Hz are situated at multiplication of index 11 i.e. [11,21,31 …..501]. Even harmonics is associated with bins with number [21,41,….501]. Odd harmonics, neglecting a fundamental component, which is localized at index 11, start from index 31 i.e. [31, 51,71…491]. According to the subdivision, we can represent now the full harmonic spectrum as well as the harmonics spectrum including even as well as odd components. The results concerning investigation of harmonics in voltage and current in dc-arc furnace plant is presented in Fig. 9.9, Fig. 9.10. The calculation of THD indices confirms predominant contribution of odd harmonics.

a) Harmonics relative to fundamental

zoom – without fundamental

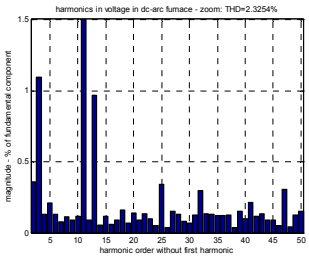

THD =

2.3254

b) Even harmonics relative to fundamental

zoom – without fundamental:

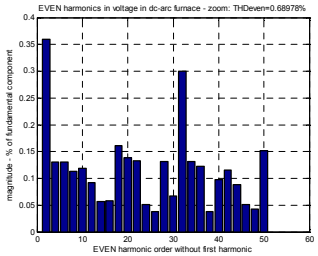

THDeven =

0.6898

c) Odd harmonics relative to fundamental

zoom – without fundamental:

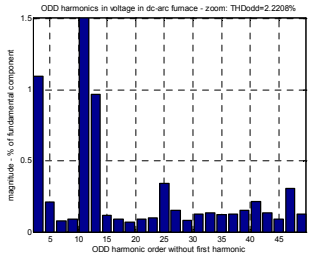

THDodd =

2.2208

Checking: $THD^2 = THDodd^2 + THDeven^2$; $THD \approx THDodd$

$2.3254^2 = 2.2208^2 + 0.6898^2$; $2.3254 \approx 2.2208$

Fig. 9.9. Harmonics analysis of voltage in dc-arc furnace plant: presentation of harmonics, THD indices calculation

a) Harmonics relative to fundamental

zoom – without fundamental

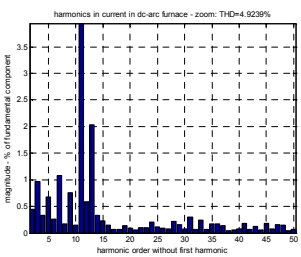

THD:

4.9239

b) Even harmonics relative to fundamental

zoom – without fundamental:

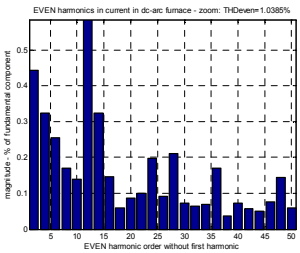

THDeven =

1.0385

c) Odd harmonics relative to fundamental

zoom – without fundamental:

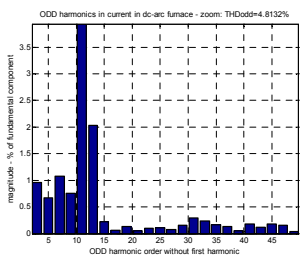

THDodd =

4.8132

Checking: $THD^2 = THDodd^2 + THDeven^2$; $THD \approx THDodd$

$4.9239^2 = 4.8132^2 + 1.0385^2$; $4.9239 \approx 4.8132$

Fig. 9.10. Harmonics analysis of current in dc-arc furnace plant: presentation of harmonics, THD indices calculation

9.5.Groups of harmonics, interharmonic and suharmonic

To deal with the new characteristics of the frequency spectra in voltage and current waveforms, the International Electrotechnical Commission (IEC) in the 2nd edition of its standard 61000-4-7 [5] has proposed the use of harmonic groups instead of the individual harmonic frequencies in order

to obtain a better estimation of harmonic distortion in modern power supply systems. The harmonic groups are defined as the grouping of the spectral bins obtained applying the Discrete Fourier Transform to the samples of voltage or current waveforms taken in rectangular sampling windows of 10 periods of the fundamental frequency in a 50-Hz system (12 periods in 60-Hz systems) and using synchronous sampling [2],[3],[4],[5].

Harmonic Group C_{hg} : in a 50-Hz system there are 9 frequency components between two harmonic orders *h* and *h + 1*. The lowest four are added to group *h*, the highest four to group *h +1*, and the middle one is divided equally between the two groups. The harmonic group ***C_{hg}*** is defined by formula:

$$C_{hg}^2 = \frac{1}{2}C_{nfch(h)-5}^2 + \sum_{i=-4}^{i=4} C_{nfch(h)-k}^2 + \frac{1}{2}C_{nfch(h)+5}^2 \qquad (9.5)$$

where *nfch(h)* means an index of harmonic order *h* in linear spectrum.

Hint: according to our previous initial calculation, ***nfch*** includes indices associated with particular harmonics in linear spectrum. e.g. nfch(1)=11 nfch(2)=21 …

Interharmonic Group C_{ihg} : All frequency components between harmonic orders *h* and *h+1* are combined in an interharmonic group:

$$C_{ihg}^2 = \sum_{i=1}^{i=9} C_{nfch(h)+k}^2 \qquad (9.6)$$

A specified interharmonic group is associated with frequencies lower than fundamental. Is is called ***subharmonic group C_{sub1g}***

$$C_{sub1g}^2 = \sum_{i=-9}^{i=-1} C_{nfch(1)+k}^2 \qquad (9.7)$$

Using the previous example of Fourier series parameterization for sampling rate 4kHz and frequency 5-Hz resolution, we can introduce the definition of the harmonic group order *h* and interharmonic group as well as a subharmonic group as it was illustrated in Fig. 9.11.

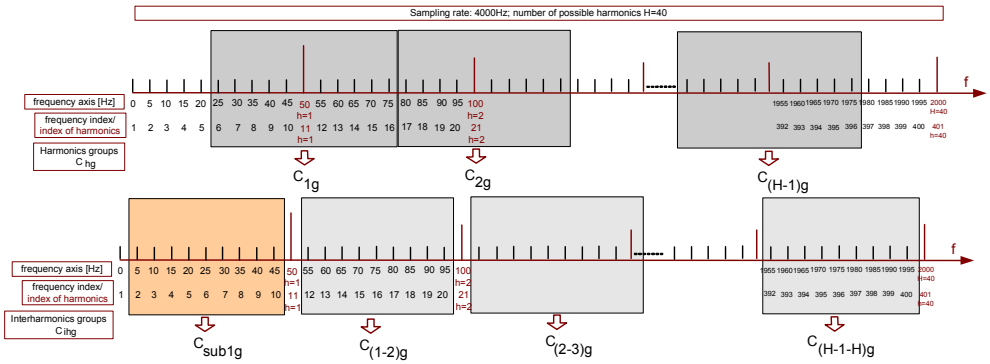

Fig. 9.11. Illustration of harmonic, interharmonic and subharmonic group definition in 50Hz system with sampling rate f_s=4kHz

In order to practice an idea of grouping the harmonics, we now encourage to define a harmonic, interharmonic and subharmonic group in case of investigated voltage in current in the dc-arc furnace plant.

Activities: Perform initial calculation to reveal frequency bins to grouping process of the harmonics.

Given: sampling rate f_S=*5kHz*, system f_0=*50Hz*, interval *10-cycle*

Aim: Selection of frequency bins in order to create a group of harmonics

Answer: An expected answer is included in the figure below, Fig. 9.12.

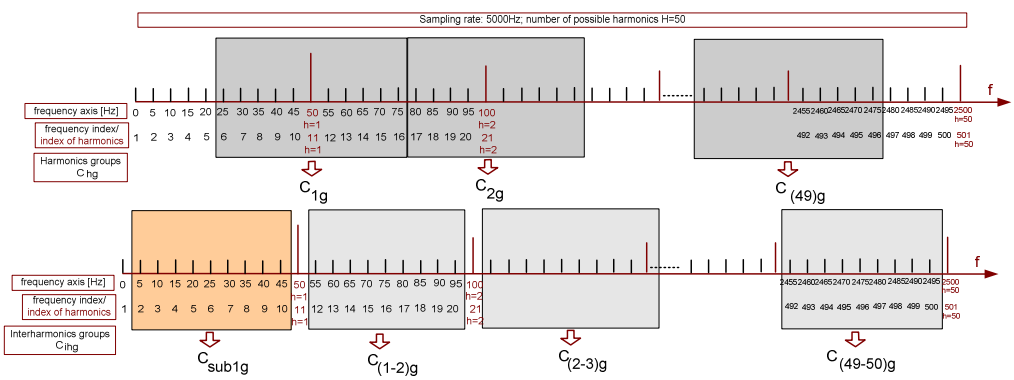

Fig. 9.12. Harmonic, interharmonic and subharmonic group definition of investigated voltage and current in example of dc-arc

The results concerning investigation of groups of harmonics in voltage in the dc-arc furnace plant is presented in Fig. 9.13. If we compare the assessment of the distortion in voltage based only on the harmonics, Fig. 9.9, we can reveal smaller values of particular components in the process of the assessment in comparison with its grouping counterpart. Discussed here an approach can have

a crucial meaning especially in presence of high value of interharmonics which in classical calculation, based strictly on harmonics, in neglected.

Fig. 9.14 represents the contribution of particular harmonics and interharmonics groups. Predominant values are concentrated around the harmonics, however, total neglecting of interharmonics, as in case of classical harmonics assessment, has a right to stay under the discussion.

a) Harmonic groups relative to fundamental
zoom – without fundamental

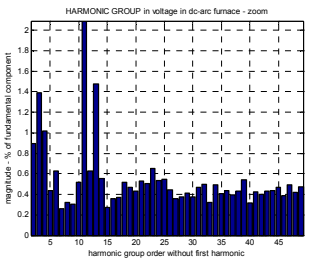

b) Interharmonic groups relative to fundamental
zoom – without fundamental:

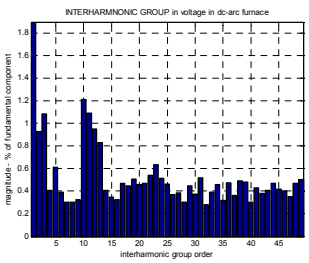

c) Subharmonic group relative to fundamental
zoom – without fundamental:

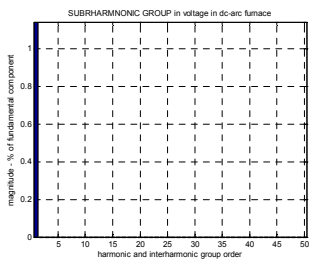

Fig. 9.13. Group of harmonics, interharmonics and subharmonic of voltage in dc-arc furnace plant

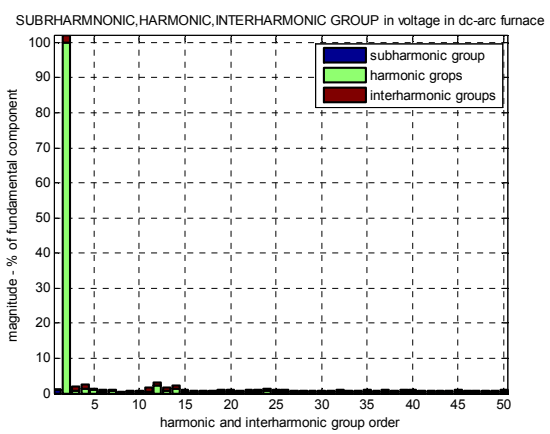

Fig. 9.14. Contribution of particular groups of harmonics, interharmonics and subharmonic of voltage in dc-arc furnace plant

Mentioned above discussion under contribution of interharmonics in assessment of the harmonic distortion has a more significant meaning in case of current, which can be much more affected by the harmonics than voltage. The level of harmonics defined as a group and as selected one frequency bin can be recognized comparing Fig. 9.15 and Fig. 9.10.

Additionally, contribution of particular harmonics and interharmonics groups are presented in Fig. 9.16.

a) Harmonic groups relative to fundamental
zoom – without fundamental

b) Interharmonic groups relative to fundamental
zoom – without fundamental:

c) Subharmonic group relative to fundamental
zoom – without fundamental:

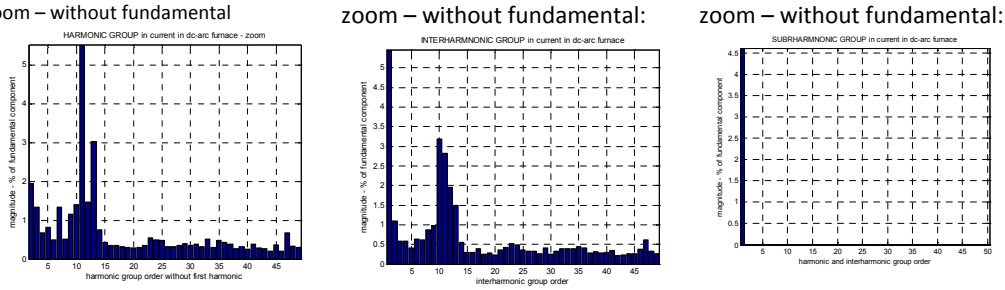

Fig. 9.15. Group of harmonics, interharmonics and subharmonic of current in dc-arc furnace plant

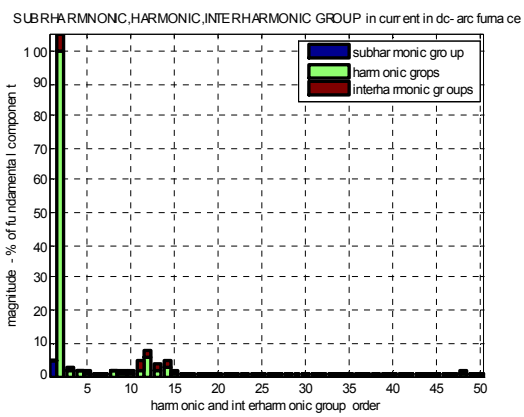

Fig. 9.16. Contribution of particular groups of harmonics, interharmonics and subharmonic of current in dc-arc furnace plant

9.6.Literature

[1] Bollen M.H.J., *Understanding Power Quality Problems. Voltage dips and interruptions*, IEE Press Series on Power Engineering, 2000.

[2] Bollen M.H.J, Irene Yu-Hua Gu, *Signal Processing of Power Quality Disturbances*, 2006 The Institute of Electronics and Electrical Engineers, Inc.

[3] *Power Quality Application Guide. Chapter 3. Harmonics*. The European Copper Institute, Leonardo da Vinci European Program on Power Quality Assessment.

[4] Electromagnetic compatibility (EMC), Part 4, Section 30: Power quality measurement methods, IEC 61000-4-30.

[5] Electromagnetic compatibility (EMC), Part 4, Section 7: General guide on harmonics and interharmonics measurements and instrumentation, for power supply systems and equipment connected thereto, IEC 61000-4-7.

[6] IEEE C37.111-1991 - IEEE Standard Common Format for Transient Data Exchange (COMTRADE) for Power Systems

[7] Bracale A., Carpinelli G., Lauria D., Leonowicz T., Lobos T., Rezmer J., *On Some Spectrum Estimation Methods for Analysis of Non-Stationary Signals in Power Systems. Part I: Theoretical Aspects, Part II – Numerical applications*, 11-th International Conference on Harmonics and Quality of Power, Lake Placid, New York 2004, Session: Harmonic Propagation, paper no. - “f” and “g.

[8] Łobos Tadeusz, Sikorski Tomasz, Schegner Peter: Joint time-frequency representation of non-stationary signals in electrical power engineering. 15th Power Systems Computation Conference - PSCC. CD-ROM Proceedings, 2005.

10. Elements of power quality report

The construction of a power quality report contains the assessment of set of many parameters discussed in this book. Recorded values are compared with recommended values. Standard contents of power quality report includes assessment of :

- power frequency
- -slow voltage variation
- fast voltage variation or flicker severity
- unbalance
- harmonics
- recorded power quality events and transients

Methodology of preparing the data base for assessment of power quality is based usually on one week assessment period. However requirements for aggregation rules, including averaging intervals, for different parameters are different [1],[2],[3].

An Algorithm for frequency estimation is based on ten-cycle series. In 50Hz systems, for every 200ms new value of frequency is stored in monitoring mode. However for assessment aggregation of 10s averaging interval is introduced, giving set of 60480 per week.

Set of frequency values in one week based on 10s aggregation:

$$1_{10s} * 6\big|_{1\min} * 60\big|_{1h} * 24\big|_{1day} * 7\big|_{1week} = 60480$$

In case of rms calculation monitoring the algorithm is based on half or one-cycle series. In the next step, 10 cycle intervals are aggregated and next averaged referring 10 min interval. The trend of voltage variation is finally based on a set of 10 min values that gives 1008 values per week:

Set of rms in one week based on 10 min aggregation:

$$1_{10\min} * 6\big|_{1h} * 24\big|_{1day} * 7\big|_{1week} = 1008$$

The calculation of unbalance coefficient and harmonics use 10-cycle interval according to requirements for Fourier series. For the assessment of 10-cycle values are averaged in 10 min as in case of rms trend. Thus, similar to slow voltage variation, a set of unbalance and harmonics is based on 1008 values per week.

Set of unbalance and harmonics in one week based on 10 min aggregation:

$$1_{10\,\mathrm{min}} * 6\big|_{1h} * 24\big|_{1day} * 7\big|_{1week} = 1008$$

Short-term flicker coefficient is stored with 10 min aggregation interval. Evaluation of voltage mitigation is defined by long-term flicker coefficient which is based on two hours averaging of 10 min short-term flicker coefficient. Thus, evaluation of flicker severity uses 84 values of long-term flicker coefficient for one-week assessment period.

Set of long-term flicker coefficient in one week based on 2h aggregation:

$$1_{2h} * 12\big|_{1day} * 7\big|_{1week} = 84$$

The mentioned rules of aggregations allows to prepare set of values in the assessment period and perform the evaluation with comparison to referring values [3].

The aim of this chapter is to present an example of power quality report including the assessment of mentioned crucial parameters. Measurements were done in the main point of the supply of the factory which has an electronic assembly line including robots and power electronics. Localisation of the power quality recorder in the distribution station of the factory presents Fig. 10.1.

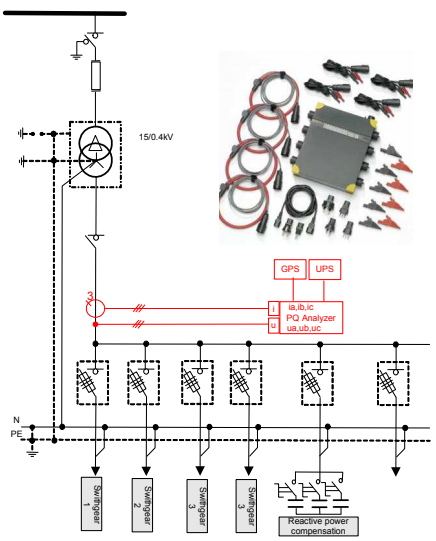

Fig. 10.1. Localisation of the power quality measurements in distribution station

10.1. Power frequency assessment

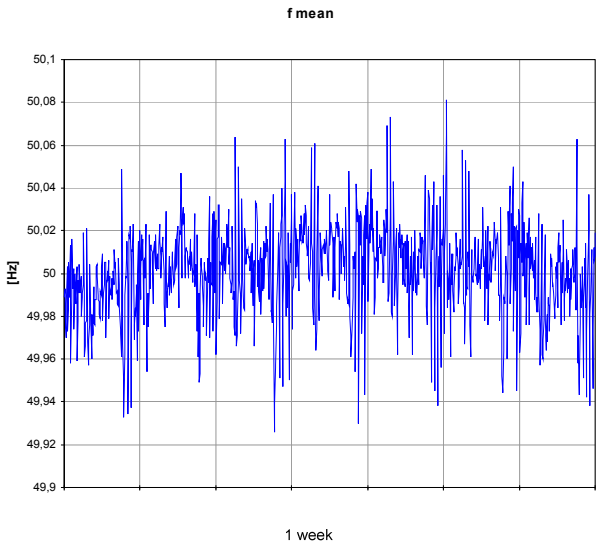

Fig. 10.2. Visualisation of power frequency variation

Table 10-1. Assessment of power frequency variation

Frequency assessment		f [Hz]
f_{10s}	***min***	***49,886***
f_{10s}	***Percentile 99.5%***	***50.055***
f_{10s}	max	50,131

Visualization of the recorded set of frequency values is shown in Fig. 10.2. The standard EN 50160 indicates that the nominal frequency of the supply voltage shall be 50 Hz. Under normal operating conditions, the mean value of the fundamental frequency measured over 10 s shall be within a range of

– for systems with synchronous connection to an interconnected system:

50 Hz ± 1 % (i.e. 49,5 Hz... 50,5 Hz) during 99,5 % of a year;

50 Hz + 4 % / - 6 % (i.e. 47 Hz... 52 Hz) during 100 % of the time;

Table 10-1 contains some statistical parameters which have confirmed that in the investigated case, requirements for frequency standards are fulfilled. During 100% of the assessment, period frequency values hold in range from 49,886 to 50,131 Hz.

10.2. Supply voltage variation

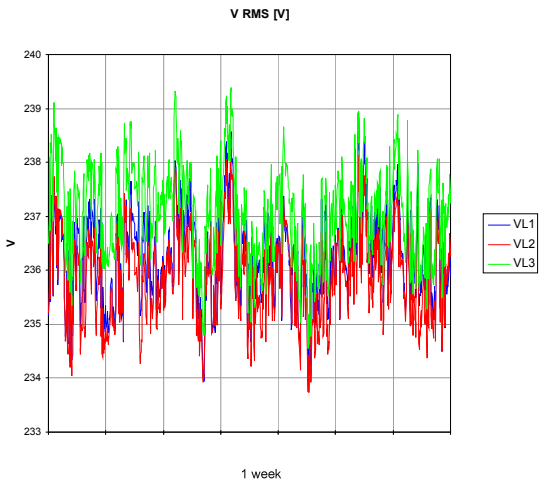

Fig. 10.3. Visualisation of supply voltage variation

Table 10-2. Assessment of supply voltage variation

Voltage assesment		VL1	VL2	VL3
		[V]	[V]	[V]
U_{10min}	***min***	***233,94***	***233,43***	***234,55***
	Percentile 95%	***237,87***	***237,51***	***238,73***
	max	238,83	238,24	239,40

Visualization of the recorded set of supply voltage values is shown in Fig. 10.3. The standard EN 50160 indicates that under normal operating conditions:

- during each period of one week 95 % of the 10 min mean r.m.s. values of the supply voltage shall be within the range of Un ± 10 %,

- all 10 min mean r.m.s. values of the supply voltage shall be within the range of Un + 10 % / - 15 %.

Table 10-2 contains some statistical parameters which have confirmed that in the investigated case requirements for rms supply voltage standards are fulfilled. 95% of the recorded rms values hold in range from 233,43V to 237,87V. Moreover, 100% of the recorded values met standard expectation.

10.3. Flicker severity

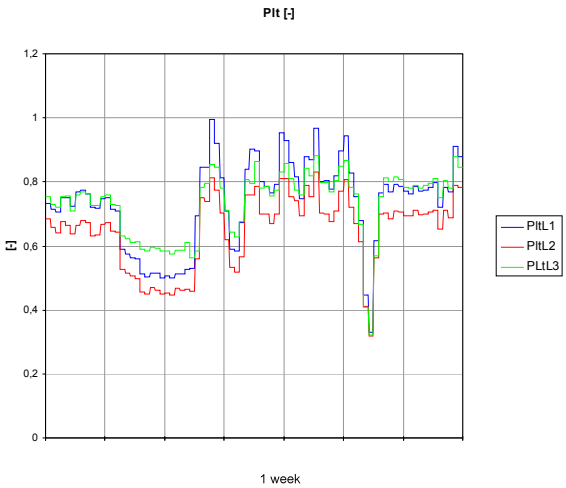

Fig. 10.4. Visualisation of long-term flicker severity

Table 10-3. Assessment of long-term flicker severity

Flicker assessment		L1	L2	L3
		[-]	[-]	[-]
Plt_{2h}	**min**	***0,33***	***0,32***	***0,32***
	Percentile 95%	***0,93***	**0,81**	***0,86***
	max	0,99	0,83	0,88

Visualization of the recorded set of long-term flicker coefficient values is shown in Fig. 10.4. The standard EN 50160 indicates that under normal operating conditions, in any period of one week the long term flicker severity caused by voltage fluctuation should be Plt ≤ 1 for 95 % of the time.

Table 10-3 contains some statistical parameters which have confirmed that in the investigated case requirements for flicker severity are fulfilled. 95% of the recorded long-term flicker values hold in range from 0,32 to 0,93. Moreover, 100% of the recorded values met standard expectation.

10.4. Voltage unbalance assessment

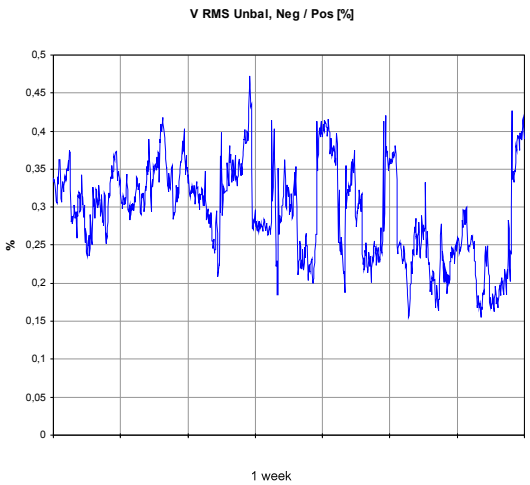

Fig. 10.5. Visualisation of unbalance variation

Table 10-4. Assessment of unbalance variation

Unbalance assesment		„Neg/Pos"
		[%]
„Neg/Pos"$_{10min}$	***min***	0,15
	Percentile95%	***0,40***
	max	0,47

Visualization of the recorded set of unbalance values is shown in Fig. 10.5. The standard EN 50160 indicates that Under normal operating conditions, during each period of one week, 95 % of the 10 min mean r.m.s. values of the negative phase sequence component (fundamental) of the supply voltage shall be within the range 0 % to 2 % of the positive phase sequence component (fundamental). In some areas with a partly single phase or two phase connected network users' installations, unbalances up to about 3 % at three-phase supply terminals occur.

Table 10-4 contains some statistical parameters which have confirmed that in the investigated case requirements for unbalance standards are fulfilled. 95% of the recorded unbalance coefficient hold in range from 0,15 to 0,40. Moreover, 100% of the recorded met standard expectation.

10.5. Harmonics assessment

Table 10-5. Assessment of harmonic variations

Harmonic assessment							
		Percentile95%			Max		
Order	Limits	L1	L2	L3	L1	L2	L3
Nr.	[%]	[%]	[%]	[%]	[%]	[%]	[%]
2	0.00 - 2.00	0.12	0.21	0.17	0.13	0.22	0.17
3	0.00 - 5.00	0.36	0.40	0.35	0.38	0.44	0.38
4	0.00 - 1.00	0.26	0.36	0.24	0.27	0.39	0.26
5	0.00 - 6.00	1.07	1.55	1.03	1.21	1.73	1.24
6	0.00 - 0.50	0.31	0.52	0.35	0.34	0.57	0.38
7	0.00 - 5.00	1.30	1.67	1.46	1.69	2.05	1.80
8	0.00 - 0.50	0.37	0.49	0.62	0.46	0.54	0.70
9	0.00 - 1.50	0.49	0.66	0.79	0.69	0.76	0.96
10	0.00 - 0.50	0.44	0.42	0.56	0.54	0.45	0.63
11	0.00 - 3.50	1.46	1.23	1.45	2.02	1.68	1.91
12	0.00 - 0.50	0.61	0.36	0.51	0.76	0.51	0.67
13	0.00 - 3.00	0.85	0.73	0.63	1.02	0.83	0.68
14	0.00 - 0.50	0.56	0.62	0.53	0.63	0.73	0.58
15	0.00 - 0.50	0.43	0.53	0.43	0.49	0.69	0.55
16	0.00 - 0.50	0.49	0.45	0.35	0.67	0.78	0.59
17	0.00 - 2.00	0.51	0.38	0.43	0.79	0.69	0.59
18	0.00 - 0.50	0.36	0.20	0.33	0.66	0.38	0.50
19	0.00 - 1.50	0.27	0.24	0.31	0.54	0.39	0.65
20	0.00 - 0.50	0.22	0.12	0.23	0.52	0.23	0.55
21	0.00 - 0.50	0.22	0.12	0.17	0.45	0.29	0.42
22	0.00 - 0.50	0.17	0.10	0.12	0.37	0.22	0.27
23	0.00 - 1.50	0.14	0.07	0.11	0.30	0.17	0.21
24	0.00 - 0.50	0.10	0.06	0.07	0.20	0.11	0.12
25	0.00 - 1.50	0.09	0.07	0.06	0.18	0.12	0.09

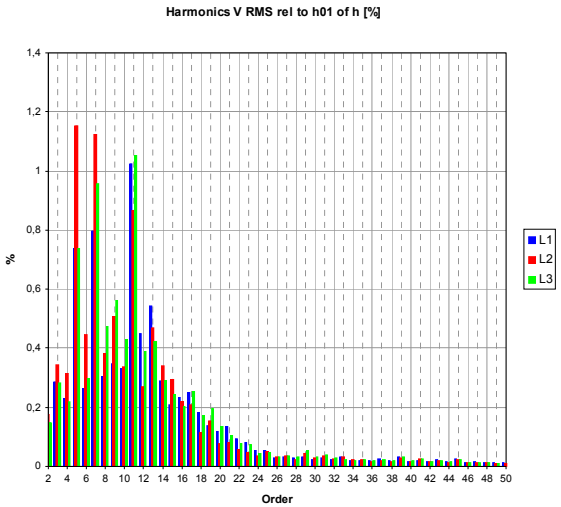

Fig. 10.6. Visualisation of harmonic spectrum averaged in one week

Table 10-5 contains limits for particular harmonics defined in EN 50160 and some statistical parameters of recorded data. Distribution of the harmonics is also visible in Fig. 10.6. Classical for LV supply network contribution of odd harmonics, especially 3-rd, 5-th, 7-th, 11-th is confirmed. There are dominated components. Performed measurements have detected values over the limits in case of even harmonics as 6-th, 8-th, 10-th,12-th,14-th. The conclusion concerning harmonics assessment is that the requirements for harmonics contribution is not fulfilled in the investigated case. Further tests shown that exceeded values appear temporary and come from resonance effects in the supply in companion with capacitor banks under process of reactive power compensation.

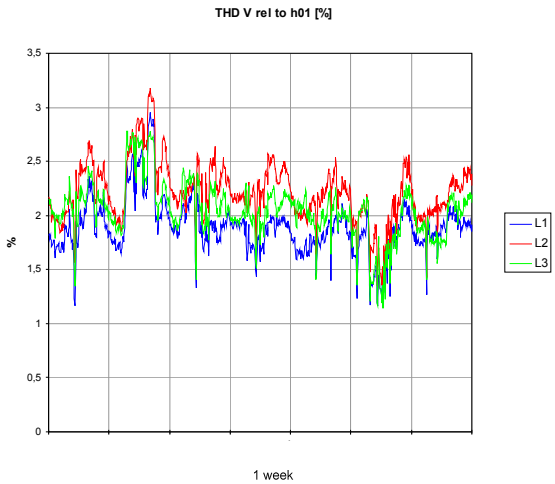

Fig. 10.7. Visualisation of THDV variation

Table 10-6. Assessment of THDV variation

THDV assesment		THDVL1	THDVL2	THDVL3
		[%]	[%]	[%]
THDV 10min	***min***	***1,16***	***1,34***	***1,14***
	Percentile95%	***2,36***	***2,68***	***2,59***
	max	2,95	3,18	2,78

Visualization of the recorded set of total harmonics distortion in voltage is shown inFig. 10.7. The standard EN 50160 indicates THD of the supply voltage (including all harmonics up to the order 40) shall be less than or equal to 8 %.

Table 10-6 contains some statistical parameters of THDV which have confirmed that in the investigated case requirements are fulfilled. 95% of the recorded THDV coefficient hold in range from 1,14 to 2,68. Moreover, 100% of the recorded values met standard expectation.

10.6. Summary of the report

Presented in the previous section, the assessment of crucial power quality parameters indicates that:

- in case of power frequency, requirements are fulfilled
- in case of voltage supply, requirements are fulfilled
- in case of flicker severity, requirements are fulfilled
- in case of voltage unbalance, requirements are fulfilled
- in case of THD of the supply voltage, requirements are fulfilled
- in case of harmonics requirements are not fulfield

Performed measurements have detected values over the limits in case of even harmonics as 6-th, 8-th, 10-th,12-th,14-th. It is recommended to make the test of the cooperation the capacitor banks with the supply during the regulation process of reactive power consumption.

During the assessment period no voltage events were detected.

10.7. Literature

[1] IEC 61000-4-30:2008, *Electromagnetic compatibility (EMC): Testing and measurement techniques -Power quality measurement method*.

[2] Bollen M.H.J, Irene Yu-Hua Gu, *Signal Processing of Power Quality Disturbances*, 2006 The Institute of Electronics and Electrical Engineers, Inc

[3] EN 50160: *Voltage characteristics of electricity supplied by public distribution networks*